Effects of microRNA-31 on skeletal muscle stem cell self-renewal *ex vivo* and *in vivo*

Heather Duncan
Degree of Master of Science
Department of Human Genetics

McGill University
Montreal, Quebec, Canada

Submitted August 2014

A thesis submitted to McGill University in partial fulfillment of the requirements of the degree of Master of Science

Dedication

This thesis is dedicated to those with Duchenne muscular dystrophy, and other myopathies, who could stand to benefit from the ongoing research in the field.

Acknowledgments

I would like to thank my supervisor, Dr. Colin Crist, for supervising my work on this project. I would also like to acknowledge the members of my supervisory committee, Dr. Janusz Rak, Dr. Aimee Ryan and Dr. Yojiro Yamanaka, for their assistance in helping me establish and approach specific research aims. I would like to thank Dr. Vahab Soleimani for serving as my external thesis examiner. I would like to thank the current and former members of Dr. Crist's lab their feedback and company; Solène Jamet, Jacqueline Chung, Victoria Zismanov, Aakritie Sareen, Victor Chichkov, Jean-Marie Jacob, Micheal Ni, Minnie Fung, and David McCusty. I would like to thank the former laboratory of Dr. Margaret Buckingham for providing Dr. Crist's lab with $Pax3^{GFP/+}$ mice. I would like to thank Dr. Michael Rudnicki and members of the Rudnicki lab for welcoming presentations of my results, and providing constructive critique. I would like to acknowledge Christian Young for training in flow cytometry and fluorescence activated cell sorting. I would like to acknowledge members of the animal core facilities at the Jewish General Hospital; Ivhans Chery for training in animal care modules, Kathy Forner for training on anaesthesia and surgical procedures, and Véronique Michaud for training on the *in vivo* imaging system. Thanks to Dr. Florian Bentzinger for providing the protocols for immunosuppression of host mice and rapid lipid-transfection of satellite cells for engraftment. Thanks to Dr. Julia von Maltzhan for providing guidance with embedding muscle samples in optimal cutting temperature compound for cryosectioning, and conducting multichannel immunofluorescence. Thanks to Dr. Penney Gilbert for providing the protocol that was implemented to detect green fluorescent protein by immunohistochemistry. I would like to thank Karine Choquet for translating my abstract to French. Finally, I acknowledge the funding awarded to Dr. Crist, which includes operating grants from Canadian Institutes of Health Research and Fonds de Recherche en Santé au Québec.

Table of Contents

List of Tables

List of Figures

were transplanted into the *tibialis anterior* muscle of immunocompromised *Foxn1$^{nu/nu}$; mdx* mice

21. Restoration of dystrophin expression after control and miR-31 transfected satellite cells, isolated from the muscle of *Pax3$^{GFP/+}$; tg(actb-luc)* mice, were transplanted into the *tibialis anterior* muscle of immunocompromised *Foxn1$^{nu/nu}$; mdx* mice
22. 4-channel immunolabeling protocol

List of Abbreviations

Ago2	Argonaute-2
β-Gal	Beta-galactosidase
BMD	Becker muscular dystrophy
BMP	Bone morphogenic protein
cDNA	Complementary deoxyribose nucleic acid
Ctrl	Control
DAPC	Dystrophin-associated protein complex
DAPI	4',6-diamino-2-phenylindole
DMD	Duchenne Muscular Dystrophy
DMD	Dystrophin gene
DMEM	Dulbecco's Modified Eagle Medium
DNA	Deoxyribonucleic acid
ECL	Enhanced chemiluminescence
EDL	*Extensor digitorum longus*
EdU	5-ethynyl-2'-deoxyuridine
FAP	Fibroadipogenic progenitor cells
FBS	Fetal bovine serum
FMRP	Fragile X mental retardation protein
FSHD	Fascioscapulohumoral muscular dystrophy
FXR	Fragile X related protein family
Fxr1	Fragile X-related protein 1
Fxr1v2	3'UTR of *Fxr1,* variant 2
Fxr1v2 mut	3'UTR of *Fxr1*, variant 2, with mutagenized miR-31 seed target site
G1	Gap 1 phase
G2	Gap 2 phase
GFP	Green fluorescent protein
HAC	Human artificial chromosome
HDAC2	Histone deacetylase 2
HEK 293	Human Embryonic Kidney 293
HEY	Hairy and enhancer of split related with YRPW
HGF	Hepatocyte growth factor
HS	Horse serum
kDa	Kilodaltons
LNA	Locked nucleic acid
LRP	Lipoprotein receptor-related protein
M.O.M.	Mouse on Mouse reagent
MCT	Muscle connective tissue fibroblasts
miR-31	MicroRNA-31
miRNA	MicroRNA
MRF	Myogenic regulatory factor

mRNA	Messenger ribonucleic acid
mRNP	Messenger ribonucleoprotein particle
Myf5	Myogenic factor 5
NaCl	Sodium chloride
NF-κB	Nuclear factor kappa-light-chain-enhancer of activated B cells
NH_4Cl	Ammonium chloride
NO	Nitric oxide
NOD-SCID	Non-obese diabetic severe combined immunodeficient
NOS	Nitric oxide synthase
OCT	Optimal cutting temperature compound
P/S	Penicillin-Streptomycin
PAGE	Poly acrylamide gel electrophoresis
Pax3	Paired-box transcription factor 3
Pax7	Paired-box transcription factor 7
PBS	Phosphate buffered saline
PCR	Polymerase chain reaction
PFA	Paraformaldehyde
Pre-miRNA	Precursor microRNA
qPCR	Quantitative polymerase chain reaction
3' RACE	3' Rapid amplification of cDNA ends
RISC	RNA-induced silencing complex
RLC	RISC loading complex
RNA	Ribonucleic acid
S phase	Synthesis phase
SC	Satellite cell
SCID	Severe combined immunodeficiency
TA	*Tibialis anterior*
TRBP	Tar RNA binding protein
TWEAK	Tumour necrosis factor-like weak inducer of apoptosis
UTR	Untranslated region
X-gal	5-bromo-4-chloro-3-indolyl-β-D-galactopyranoside
µL	Microlitre
µm	Micrometre

Abstract

Duchenne muscular dystrophy is a heritable myopathy resulting in progressive muscle weakness and atrophy, reducing life expectancy to 20-30 years. Degeneration is caused by the virtual lack of dystrophin, a protein involved in the structural integrity of muscle fibres. Satellite cells, the adult stem cells responsible for all post-natal growth and regeneration of skeletal muscle, are a possible source of donor cells for treatment of Duchenne muscular dystrophy. *Ex-vivo* culture of satellite cells causes differentiation into myoblasts. Transplanted myoblasts may contribute to dystrophin restoration, but are not capable of self-renewal and homing to the satellite cell for subsequent rounds of regeneration. This work aims to investigate the role of the microRNA-31 in self-renewal of satellite cells *ex vivo* and *in vivo*. MicroRNA-31 targets the myogenic factor 5 (*Myf5*) transcript to impede expression of this myogenic regulatory transcription factor, opposing the differentiation cascade. Transfection with microRNA-31 increased the proportion of cultured satellite cells expressing the transcription factor PAX7, and lacking expression of the myogenic regulatory factor MYOD *in vitro*. This indicates a cell phenotype associated with self-renewal of satellite cells, as opposed to differentiation. Effects of microRNA-31 on accumulation of MYOD may be mediated by downregulation of FXR1, an RNA-binding protein implicated in stabilization of MYOD expression. Conversely, it was demonstrated that miR-31 does not influence the proliferation rate of satellite cells *in vitro*. An engraftment assay was performed in nude-*mdx* mice to determine the effects of miR-31 *in vivo*. Transient transfection of donor-derived satellite cells with miR-31 prior to engraftment did not have a statistically significant effect on their *in vivo,* analyzed by bioluminescence imaging, restoration of dystrophin expression or their self-renewal of donor-derived satellite cells.

Abrégé

La dystrophie musculaire de Duchenne est une forme de myopathie héréditaire qui mène à une atrophie et une faiblesse musculaire progressive, réduisant ainsi l'espérance de vie des patients à environ 20-30 ans. La dégénérescence est causée par l'absence de dystrophine, une protéine impliquée dans l'intégrité structurale des fibres musculaires. Les cellules satellites sont des cellules souches adultes responsables de la croissance post-natale et de la régénération des muscles squelettiques. Elles sont également une source potentielle de cellules donneuses pour le traitement de la dystrophie musculaire de Duchenne. La culture de cellules satellites ex vivo entraine leur différenciation en myoblastes. Lors de la transplantation de myoblastes, ceux-ci peuvent contribuer à rétablir l'expression de la dystrophine, mais ils sont incapables de s'auto-renouveler ou de retourner vers l'état de cellule satellite pour permettre des cycles de régénération supplémentaires. L'objectif de ce projet est d'étudier la voie de signalisation des microARNs afin de réguler le renouvèlement des cellules satellites ex vivo et in vivo. Le microARN-31 cible l'ARN messager myogenic factor 5 (Myf5) afin de réprimer l'expression de ce facteur de transcription myogénique et de s'opposer à la cascade de différenciation. La transfection du microARN-31 augmente la proportion de cellules satellites en culture exprimant le facteur de transcription PAX7 et n'exprimant pas le facteur myogénique régulateur MYOD. Ces résultats sont caractéristiques d'un phénotype cellulaire associé au renouvèlement des cellules satellites, et non à leur différenciation. L'effet du microARN-31 sur l'expression de MYOD pourrait être modulé par la sous-expression de FXR1, une protéine liant l'ARN impliquée dans la stabilisation de l'expression de MYOD. Au contraire, nos résultats démontrent que miR-31 n'influence pas le taux de prolifération des cellules satellites in vitro. Nous avons effectué une expérience de greffe dans des souris mdx dépourvues de système immunitaire acquis afin de déterminer les effets de miR-31 in vivo. La transfection transitoire de miR-31 dans des cellules satellites donneuses n'a pas d'effet statistiquement significatif sur l'expansion des cellules dérivées de donneuses, tel qu'analysé par imagerie bioluminescente in vivo. Une telle transfection n'a pas non plus d'effet sur la restauration de l'expression de la dystrophine ou sur l'auto-renouvellement in vivo.

Introduction

Skeletal Muscle

Three distinct types of muscle tissue exist in mammals: smooth muscle, cardiac muscle, and skeletal muscle[1]. Skeletal muscle is responsible for voluntary movement and the maintenance of upright posture[1]. The long multinucleate cells that make up skeletal muscle tissue are called muscle fibres, or myofibres[2, 3]. The sarcolemma is the skeletal muscle cell's membrane, while the cytoplasm of myofibres is termed the sarcoplasm[2, 3]. In place of an endoplasmic reticulum, myofibres contain sarcoplasmic reticulum[2, 3].

The endomysium is the innermost layer of connective tissue, which surrounds each myofibre[2, 3]. Myofibres are grouped into fascicles, which are held together by another connective tissue layer called the perimysium[2, 3]. A network of blood vessels run between the fascicles and enter the bundles to connect each myofibre to the vasculature[2, 3]. The outermost layer of connective tissue surrounding each skeletal muscle is called the epimysium[2, 3]. The various layers of connective tissue converge at the extreme ends of skeletal muscles to produce the tendons, where skeletal muscles attach to the bones of the skeleton by myotendinous junctions (Figure 1)[2, 3].

Skeletal muscles enable voluntary movement by contracting to exert force on the skeleton at the tendon's insertion point adjacent to a moveable joint. Axon branches from motor neurons associate with each myofibre at interfaces called neuromuscular junction[2, 3]. Contraction is initiated when the axon of a motor neuron releases the neurotransmitter acetylcholine into the synaptic cleft[3]. The contractility of skeletal muscle tissue is central to its function in the maintenance of upright position, respiration, and locomotion[3].

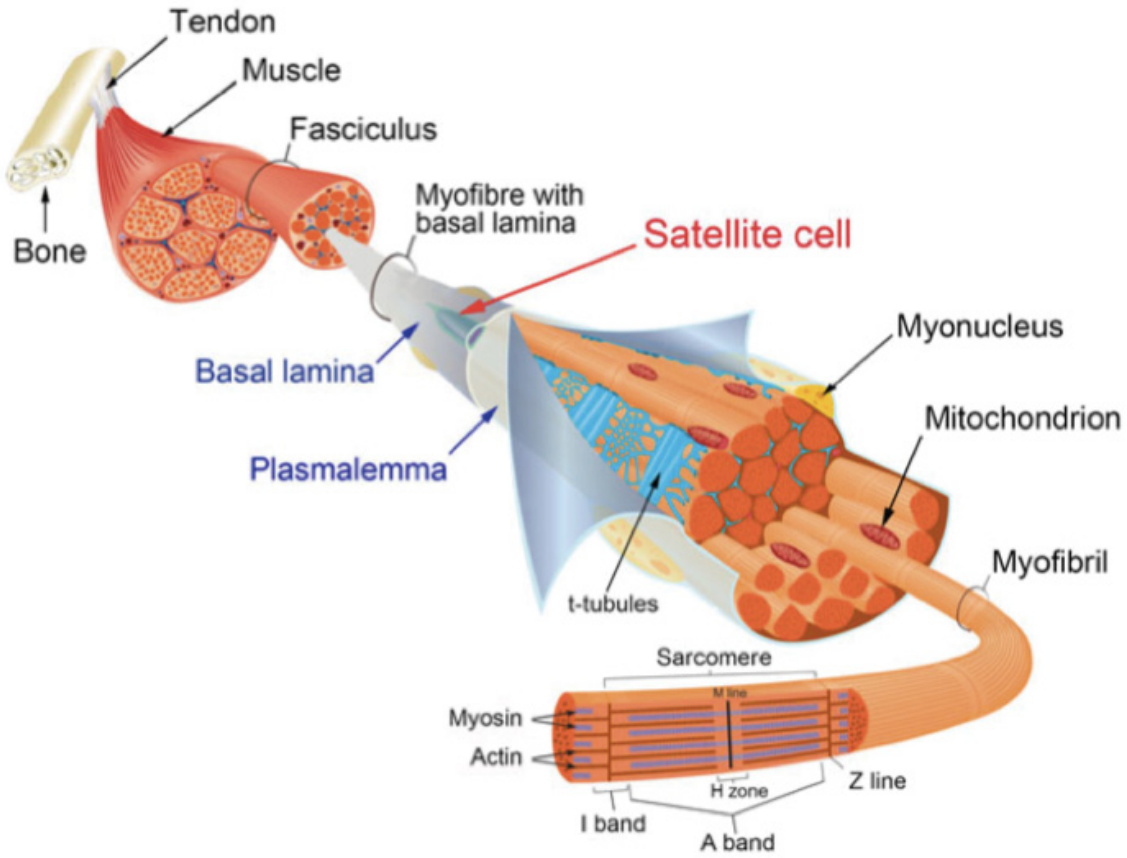

Figure 1: Anatomy of skeletal muscle tissue. The red arrow points out the satellite cell position between the sarcolemma and basal lamina of the myofibre. Image obtained from Relaix, F. and Zammit, P.; Development, 2012[4].

Satellite Cells

Development

Skeletal muscle tissue originates from the somites during embryonic development. Epithelium from the somite gives rise to the dermomyotome, which forms along the dorsal side of the embryo[5]. Cells of the dermomyotome delaminate and differentiate into myocytes, contributing the initial scaffold of the myotome[5]. Epithelial cells from the central domain of the dermomyotome undergo epithelial to mesenchymal transition to yield muscle progenitor cells, which migrate to populate the myotome which becomes skeletal muscle tissue[5]. The muscle progenitor cells proliferate, promoting growth of skeletal muscle tissue, until about day 16 of embryonic development in mice[5]. At this point, the muscle progenitor cells localize to the satellite cell position, between the

sarcolemma and basal lamina of muscle fibres[5]. Genetic tracking and somite grafting experiments have identified this lineage as the origin of satellite cells in postnatal muscle[5]. Satellite cells are the adult stem cells responsible for all post-natal regeneration of skeletal muscle[5]. Satellite cells meet the criteria of stem cells, in that they are able to self-renew as well as differentiate[6].

Self-Renewal

Satellite cells are rare, comprising only 2-5% of nuclei in skeletal muscle tissue[7, 8]. They can be identified by the expression of paired-box transcription factor 7 (PAX7), a member of the paired-box family of transcription factors involved in commitment to various tissue types during embryonic development[9]. PAX7 marks commitment to the myogenic lineage, and is essential for satellite cells to initiate myogenesis[9].

PAX7 is also crucial for the self-renewal capacity of satellite cells[10]. *Pax7* knockout mice die at 2-3 weeks of age, due to progressive ablation of cells in the satellite cell compartment due to abortive mitosis[11, 12]. This is accompanied by a reduction in myonuclei number, myofibre diameter, and muscle mass[11, 12]. Inducible ablation of *Pax7* in adult mice results in failure to regenerate damaged muscle, demonstrating that PAX7+ satellite cells are absolutely necessary for regeneration of muscle tissue following injury in vivo[10, 13].

Paired-box transcription factor 3 (*Pax3)* is a paralog of *Pax7*[12]. The myogenic progenitor cells of the embryo, which give rise to satellite cells, are positive for both PAX3 and PAX7[5]. PAX3 and PAX7 differ in their ability to regulate target genes[9, 12]. Whereas PAX7 is required for postnatal myogenesis, PAX3 is more critical during embryonic development[11, 12, 14]. PAX3 expression peaks as muscle progenitor cells delaminate from the somite, and migrate to the limb buds[12]. PAX3 is generally downregulated in satellite cells after birth, except in a subset of muscles including trunk region[12]. *Pax3*-null mice lack limb muscles, whereas *Pax7*-null mice have relatively normal development of skeletal muscle but virtually lack any capacity for regeneration[12]. PAX3+ satellite cells from diaphragm of *Pax7*-null mice are capable of forming myotubes with reduced efficiency[12].

Myogenesis

PAX7 functions upstream of a family of transcription factors called the myogenic regulatory factors (MRFs)[11]. Myogenic regulatory factors (MRFs) are a group of basic helix-loop-helix transcription factors specific to skeletal muscle tissue[15, 16]. They include MYF5, MYOD, myogenin, and MRF4[16]. Expression of MYF5 indicates commitment of PAX7+ satellite cells to the myogenic lineage[9]. A subpopulation of satellite cells, called satellite reserve cells, is naïve for expression of MYF5[17]. Satellite reserve cells make up approximately 10% of the PAX7+ cells under the basal lamina of muscle fibres[17]. Satellite reserve cells self-renew by asymmetric cell division, giving rise to a daughter reserve cell and daughter cells that translates MYF5[17]. Upon transplantation, reserve PAX7+/MYF5- satellite cells have been shown to migrate and engraft in the surrounding tissue, while PAX7+/MYF5+ satellite cells remain at the site of injection[17].

Chromatin remodelling by the PAX7 complex activates the *Myf5* transcript[9]. *Pax7*-null satellite cells are devoid of MYF5 expression[9]. Conversely, exogenous expression of PAX7 in C2C12s increases the levels of *Myf5* transcript and *Myf5* protein[9]. In satellite cells, *Myf5* is sequestered into messenger ribonucleoprotein particles (mRNPs) in which they are stored for later translation[18]. As satellite cells activate from quiescence, the mRNP granules dissociate and release *Myf5* to rapidly enter the polysome for translation[18]. *Myf5* plays a role in the activation and proliferation of satellite cells[19]. Adult *Myf5* knockout mice suffer from a mild progressive phenotype with impaired skeletal muscle regeneration[19]. Their phenotype is exacerbated upon injury or aging, resulting in myofibre hypertrophy, and infiltration of skeletal muscle by adipose and fibrotic tissue[19].

Myofibres are subject to mechanical stress due to routine use, as well as acute injury, both of which result in structural damage[20]. Mechanical damage of myofibres leads to necrosis, which attracts inflammatory cells to the area and signals the release of trophic factors[21]. These factors stimulate activation of satellite cells[21]. Activated satellite cells are PAX7+/MYOD+[17, 22, 23]. They can repress MYOD expression while maintaining PAX7 in order to return to quiescence[4, 17, 22]. Conversely, downregulation of PAX7 marks differentiation into myoblasts, which are committed to terminal differentiation to form muscle fibres[24]. PAX7 and MYOD have been described as key

regulators of the balance between self-renewal and differentiation of satellite cells[19]. Proliferating satellite cells undergo symmetric and asymmetric divisions[24], forming a heterogeneous myocolony along the myofibre, including satellite cells and myoblasts[17].

Myoblasts that have differentiated from satellite cells are PAX7-/MYOD+[17, 22, 23]. Growth factors, including nerve growth factor, insulin-like growth factor-1, and basic fibroblastic growth factor induce myoblast proliferation[20]. Myoblasts give rise to muscle precursor cells, which fuse to repair or replace damaged myofibres (Figure 2)[6, 25, 26]. Myonuclei are positioned around the perimeter of myofibres, rather than throughout their cross-sectional area[2]. The cross-sectional area of a muscle fibre is closely related with the number of myonuclei it contains, suggesting that each myonuclei contributes a set amount of cellular material within a myofibre[27, 28].

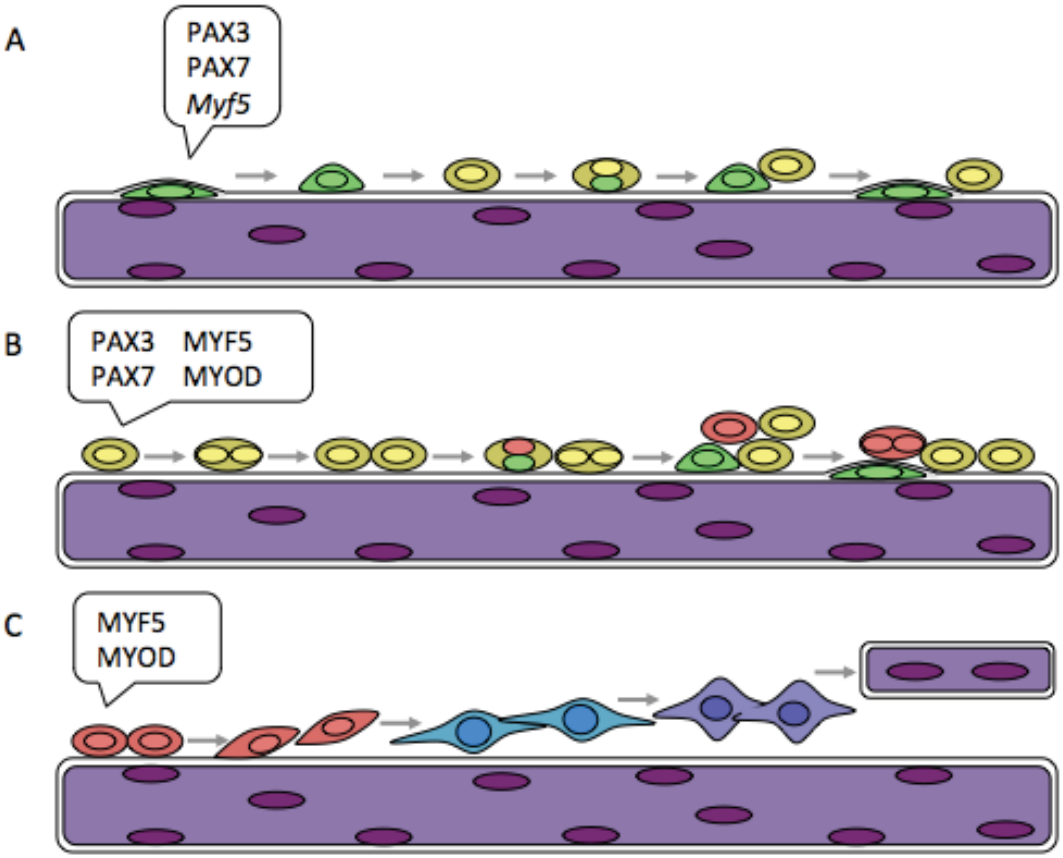

Figure 2: The myogenic program. A) Quiescent satellite cells express PAX7, PAX3 in a subset of muscles, and the *Myf5* transcript upon re-entry into the cell cycle. In response to injury, they delaminate and activate, but are still capable of self-renewal and replenishing the satellite cell niche. B) Activated satellite cells express PAX7, and PAX3 in a subset of muscles, as well as MYF5 and MYOD. They can proliferate to form a heterogeneous myocolony, containing self-renewing satellite cells and differentiating myoblasts. C) Myoblasts have lost expression of PAX7 and PAX3, and are incapable of self-renewal or homing to the satellite cell niche. They are committed to differentiation along the myogenic lineage to regeneration myofibres.

Satellite Cell Niche

The term "niche" was first used by Dr. R Schofield to describe the importance of the microenvironment surrounding stem cells[29]. It was hypothesized that cues from the niche preserve self-renewal, and that stem cells would lose their stem cell identity if removed from their niche[29]. Satellite cells reside outside the sarcolemma but beneath the basal lamina of each muscle fibre[6]. This niche supports the quiescence of satellite cells.

Satellite cells dissociated from their niche retain their capacity to regenerate skeletal muscle upon transplantation into a host microenvironment[30]. Satellite cells

obtained from young and aged donors have been shown to engraft and initiate myogenesis upon transplantation into young hosts[30]. Conversely, engraftment of satellite cells from young or aged donors is diminished in aged hosts, emphasizing the importance of the host microenvironment in satellite cell engraftment assays[30]. Parabiosis experiments in mice have revealed that circulating factors from young mice improve the efficiency of skeletal muscle regeneration in aged mice[31].

Non-myogenic cell types are an important contributor to the satellite cell niche. Outside the basal lamina that surrounds each myofibre, proliferating myoblasts come in contact with inflammatory and stromal cells[32]. Chronic degeneration of skeletal muscle tissue is often met with infiltration of white adipocytes and fibrous tissue[32]. These cells arise from bipotent fibro-adipogenic progenitor cells (FAPs), which proliferate in response to muscle damage[32]. The transiently expanded FAP population modulates the microenvironment to support myogenesis. Co-culture of myogenic progenitors with FAPs increases activation of myogenin and *MyoD* transcripts, and decreases *Pax3* and *Pax7* transcripts[32]. During regeneration of skeletal muscle, muscle connective tissue fibroblasts (MCTs) transiently increase in numbers and surround myofibres[33]. Satellite cells and MCTs undergo reciprocal interactions, which support muscle regeneration[33]. Ablation of muscle connective tissue fibroblasts leads to premature differentiation of satellite cells, and small cell sizes[33].

Duchenne Muscular Dystrophy

Pathophysiology

Duchenne muscular dystrophy (DMD) is an X-linked recessive disorder, affecting 1 in 3500 males and an estimated 1 in 50,000,000 females at birth[34, 35]. DMD is caused by a mutation truncating the dystrophin protein[36]. These mutations consist of point mutations introducing a premature stop codon, or a frameshift mutations leading to premature termination of translation[37]. Approximately 35% of cases are caused by a somatic mutation, rather than inheritance[35].

In the absence of dystrophin, muscle fibres are vulnerable to structural damage[38]. A chronic cycle of degeneration and regeneration ensues[39]. Eventually the self-renewal capacity of satellite cells is exhausted, and their numbers begin to decline[39]. Subsequent degeneration is met with degeneration of muscle tissue, as well as inflammation, fibrotic infiltration and oxidative stress[38]. Boys with DMD typically require a wheelchair by age 12, and suffer premature death at around 30 years of age[40-42], caused by heart and respiratory failure[39]. Currently there is no effective cure, only palliative therapies[36].

Somatic reversion mutations and alternative splicing occasionally restore the open reading frame of the dystrophin gene, resulting in dystrophin expressing revertant fibres occurring at a rate of 0.01% - 7% of all fibres in DMD patients[43]. Revertant fibres are thought to arise from reversion mutations in satellite cells, and have been shown to increase at a clonal level with age[37]. The number of revertant fibres per cross sectional area does not significantly increase with age in cardiac muscle, which lacks satellite cells, or in the absence of regeneration of skeletal muscle[37]. Revertant fibres in mdx mice expression dystrophin in limited number of nuclear domains, spanning up to 900μm or more typically 100μm-300μm longitudinally[37]. Since revertant fibres only express dystrophin in patches along their length, they are not protected from damage to the sarcolemma[37]. In fact, the rate of revertant fibres does not impact the clinical severity of the disease[37].

Current Treatment

Current therapy for DMD patients includes a course of glucocorticoids to slow the loss of muscle function[40, 44]. These drugs inhibit inflammation and suppress immune activity, which leads to a microenvironment that less rapidly exhausts the endogenous satellite cell pool[44]. Because glucocorticoids regulate expression of many genes, there are many off-target effects of glucocorticoid administration[44]. Several other drugs have been used to prevent inflammation and promote regeneration, including nitric oxide (NO), anti-myostatin antibodies, and histone-deacetylase inhibitors[40]. Respiratory and physical therapy are also important for patients with DMD[45]. So far, no therapeutic approach has been able to prevent progression of DMD over time[40].

Approaches for Therapy

Gene Therapy

Exon skipping

One of the therapeutic strategies undergoing clinical trials is antisense oligonucleotide mediated exon-skipping therapy[43]. Due to the vast variation of causative mutations exists among DMD patients; the clinical application of single exon skipping would be an example of personalized medicine[46, 47]. Skipping of exon 51 is useful in 10% of DMD patients; skipping of exons 45, 52, 53 and 55 is relevant to 28% of patients[47]. In order to direct therapy towards a larger proportion of DMD patients, the exon 45-55 region can be skipped. This region covers many of the most common mutation sites causing DMD, and would provide restoration of protein expression in 40-45% of DMD patients[47].

The dystrophin protein resulting from exon skipping is internally truncated, lacking a portion of the linker region, but retains domains involved in binding to the cytoskeletal and associating with the dystrophin-associated protein complex (DAPC)[47]. Similarly, patients with Becker muscular dystrophy (BMD) have in-frame internal truncations of dystrophin[47]. BMD patients exhibit a much milder phenotype and survive to old age[47]. An important consideration in the development of an antisense oligonucleotide therapy is the balance between targeting more causative mutations and retaining a functional dystrophin protein. Nonetheless, wider exon skipping therapy is more amenable to clinical use due to the reduced cost per patient[47]. Antisense oligonucleotides are increasingly considered as therapeutic approaches for other forms of muscular dystrophy; including limb-girdle muscular dystrophy, myotonic muscular dystrophy, and Fukuyama muscular dystrophy[40].

Delivery of gene therapy can be mediated through adeno-associated virus, which has high infection efficiency and specificity towards skeletal muscle[40, 48]. Restoration of dystrophin expression by adeno-associated virus delivery of exon-skipping oligonucleotides was associated with restoration of miR-31 levels in whole muscle towards wildtype levels[38]. Since the dystrophin gene is too long to load into the viral backbone,

researchers have produced a mini-dystrophin gene[43]. Mini-dystrophin is translated into an internally truncated dystrophin protein, similar to that produced by exon skipping[43].

Read-Through

Read-through strategies are an alternative to exon skipping. Changes are made to the conformation of mRNA structure using small molecule administration, which leads to replacement of the premature stop codon with another amino acid[40]. Clinical trials have been conducted to study the effects of a read-through inducing drug, PTC124, which was named Ataluren[40]. This drug is targeted to the mutation causing less than 10% of DMD cases[49]. The phase I trials have demonstrated the safety of this drug, however phase IIa trials in DMD and BMD patients have not identified an improvement in muscle function[40]. Ataluren has also been shown to induce exon skipping of the dysferlin gene in a patient with Limb Girdle Muscular Dystrophy 2B[40].

Gene Replacement

Full-length dystrophin can be encoded in a human artificial chromosome (HAC). HACs are episomal vectors containing telomeres, centromeres, and origins of replication to mimic the structure of a chromosome[40]. The cell maintains HACs during mitosis, and the copy number of the cloned gene is not altered[40]. The major advantage over cloning into other vectors is the complete lack of size restrictions[40]. The entire 2.4 megabase dystrophin locus, including promoters and regulatory elements, have been successfully cloned into a HAC[40]. HAC-dystrophin has been transferred into mesoangioblasts, which have been transplanted into severe combined immunodeficient (SCID) *mdx* mice. This resulted in engraftment of donor cells, reduced fibrotic and adipose infiltrate, and increased muscle strength[50].

Upregulation of Utrophin

Utrophin is another protein capable of taking the place of dystrophin in the DAPC. One concern in utrophin upregulation and mini-dystrophin therapy is preserving the binding site for NO synthase (NOS). NOS binds to dystrophin within the central region in which most mutations occur[44]. In its absence, NOS localizes to the cell surface, which may have a role in the dystrophic phenotype[44]. The dystrophin/NOS pathway controls

the oxidoreductase state of muscle following injury[38]. NOS is important for homeostasis of calcium ions, which plays a role in contraction of skeletal muscle[36]. NO signalling is involved in the regulation of microRNAs important in regulating myogenesis[38]. Overexpression of neuronal nitric oxide synthase has helped alleviate the dystrophic phenotype of *mdx* mice[44].

Cell Therapy

Myoblast Transplantation

As early as 1989, myoblast transplantation experiments were conducted, and resulted in restored dystrophin expression upon transplantation into immunodeficient dystrophic muscle[11]. Upon fusion to host myofibres, normal myoblasts lead to the production of full-length dystrophin in resulting chimeric myofibres, analogous to the patchy dystrophin expression caused by random X-chromosome inactivation in carriers of DMD[15, 51]. This procedure was translated into several clinical trials in the early 1990's, despite controversy over whether sufficient studies had been done in animal models[11, 52]. Little therapeutic benefit was achieved in these studies[52].

In 1991, Huard *et al.* detected dystrophin-positive fibres in transplant recipients, but they could not be distinguished from revertant fibres[11, 53]. In 1993, Tremblay *et al.* published results of a myoblast transplantation trial in boys with DMD, demonstrating that the transplanted myoblasts triggered an immune response which destroyed donor-derived myotubes, warranting the use of immunosuppressant drugs in future clinical trials[54]. In 1993, Karpati *et al.* reported a study with no adverse effects; however only one of the eight participants had dystrophin expression 5% of normal[55]. Additionally, there was no evidence of donor DNA or RNA[55]. Later it was determined that cyclophosphamide, the immunosuppressant used by Karpati *et al.*, results in lysis of donor-derived myotubes and is associated with adverse effects with long-term use[11, 56]. Gussoni *et al.* detected normal dystrophin transcript by reverse transcriptase polymerase chain reaction (PCR) but no increase in dystrophin positive fibre[51]. Mendell *et al.* obtained dystrophin of donor origin in 10% of fibres in one patient[57].

A likely explanation for the inability of myoblasts to contribute efficiently to regeneration upon transplantation is rapid cell death. Myoblast transplantation into both

mdx and wildtype (C57Bl6) mice has resulted in killing of approximately 85% of cells within minutes of injection[58]. One explanation for this is the effect of complement 3[58].

Satellite Cell Transplantation

More recently, the field has returned to studying the effects of cell therapy in animal models[52]. Satellite cells are an attractive cell type for cell therapy to treat muscular dystrophy due to their physiological adult stem cell role in skeletal muscle tissue. Tracking of donor cells from *Myf5-nLacZ/FLuc* transgenic mice demonstrated a decline in transplanted myoblasts decline, in contrast to an approximate 60-fold expansion of transplanted quiescent satellite cells[59].

Transplanted satellite cells are capable of engrafting into host muscle by entering the niche under the basal lamina, and continuing to express PAX7, indicating self-renewal[30]. Engraftment of wildtype or genetically corrected satellite cells provides a functional copy of the dystrophin gene, which will disseminate throughout the muscle as the satellite cells contribute to regeneration, addressing the initial cause of the dystrophic phenotype.

Based on the rapid decline in transplanted myoblasts, survival of transplanted satellite cells is an important concern. Poor survival can be somewhat overcome by transplanting more cells[11]. However, the rarity of satellite cells makes isolation of large numbers by flow cytometry expensive and time-consuming. Furthermore, in the event of transplantation of satellite cells from matched donors for human therapy, a minimally invasive muscle biopsy procedure would be sought after[60]. *Ex-vivo* expansion could overcome these limitations of cell therapy, as well as immune rejection of donor cells, poor cell survival, and limited spread following transplantation[15].

Transplantation of Other Cells

C2C12s an immortalized line of myogenic cells that rapidly differentiate into myotubes in culture[61]. C2C12s are not a candidate for engraftment assays in vivo due to extensive tumour formation by many clones[61]. Foetal skeletal muscle progenitors have also been used in transplantation assays into dystrophic muscle; however, the regenerative ability of foetal myogenic progenitors was found to be inferior to that of satellite cells[62].

Mesoangioblasts are a stem cell population derived from pericytes within the muscle, which are capable of crossing the epimysium following transplantation by intra-arterial injection[63]. This allows mesoangioblasts to engraft systemically, whereas satellite cells can only engraft in the muscle into which they are transplanted. Since mesoangioblasts are rare in limb-girdle muscular dystrophy patients, fibroblasts and myoblasts were collected and reprogrammed to produce induced pluripotent stem cells[63].

Originally taken as fibroblasts and myoblasts from limb-girdle muscular dystrophy patients, the induced pluripotent stem cells were genetically corrected ex-vivo using a lentiviral vector encoding human alpha-sarcoglycan complementary DNA (cDNA) under the promoter and enhancer of myosin light chain, which is muscle specific[63]. Following intramuscular and intra-arterial transplantation into alpha-sarcoglycan-null immunodeficient mice, these cells have restored alpha-sarcoglycan expression and demonstrated superior engraftment compared to fibroblasts or myoblasts[63]. A comparison remains to be done to determine the engraftment efficiency of mesoangioblasts-like cells versus satellite cells.

Myogenic Progenitors from Pluripotent Stem Cells

"Satellite-like" cells have been generated from mouse embryonic stem cells. This was done in concentrated hanging drop culture in differentiation medium, consisting of Dulbecco's Modified Eagle Medium (DMEM) with penicillin/streptomycin (+P/S), 0.1mM nonessential amino acids, 0.1mM 2-mercaptonethanol, 5% horse serum (HS), and 10% fetal bovine serum (FBS)[26]. These cells have been shown effective in in vivo engraftment assays and repopulation of the satellite cell niche between the basal lamina and sarcolemma with PAX7+ donor derived cells[26]. Likewise, satellite-like cells have been generated from induced pluripotent stem cells[60]. Satellite-like cells derived from human induced pluripotent stem cells have also engrafted as PAX7+ cells under the basal lamina of myofibres in NOD-SCID gamma-c mice, the model commonly used to study hematopoietic stem cell transplant[60].

Differentiation of satellite cells from induced pluripotent stem cells is a less invasive alternative to obtaining satellite cells from a skeletal muscle biopsy. Further advancement

of the field is required to ensure that satellite-like cells behave like satellite cells in vivo over the long term, without tumour formation. If satellite-like cells from induced pluripotent stem cells were to be used in autologous cell therapy to treat DMD, gene therapy would also be required to enable expression of dystrophin upon engraftment.

Ex-vivo Expansion of Satellite Cells

Approaches for cell therapy to treat DMD include *ex-vivo* genetic correction of the *DMD* gene of autologous satellite cells for re-implantation into the patient, and transplantation of satellite cells from matched donors without mutations in *DMD*[39]. A major difficulty in satellite cell engraftment therapy has been *ex-vivo* expansion of satellite cells capable of self-renewal[39]. Culture of satellite cells on plastic culture plates leads to differentiation, preventing satellite cells from contributing to the satellite cell compartment following transplantation into dystrophic muscle[64, 65]. Several groups are attempting to mimic microenvironment cues from the satellite cell niche to maintain self-renewal of satellite cells in culture.

One method that has been used to address this problem is activation of Notch signalling by culturing canine satellite cells on plates coated with Delta-1^{ext}-IgG, the extracellular domain of the Notch ligand Delta-1 fused to the Fc (Fragment, crystallisable) portion of human immunoglobulin G (IgG)[66]. Delta-1^{ext}-IgG cultured cells have been transplanted into irradiated, non-obese diabetic severe combined immunodeficient (NOD-SCID) mice, in which muscle was induced into regeneration by injection with barium chloride. Engraftment of Delta-1^{ext}-IgG cultured satellite cells, measured by dystrophin positive fibres, and PAX7+ satellite cells of donor origin, approached the efficiency of freshly isolated satellite cells[66].

The cytokine TWEAK (tumour necrosis factor-like weak inducer of apoptosis) and its receptor, fibroblast growth factor inducible 14, are increased in skeletal muscle following injury[67]. TWEAK represses the Notch pathway and activates the nuclear factor kappa-light-chain-enhancer of activated B cells (NF-κB) cell signalling pathway[67]. This leads to a reduction in the proportion of PAX7 positive satellite cells capable of self-renewal[67]. Following injury, TWEAK knockout mice have more PAX7+ satellite cells[67]. Blocking of NF-κB signalling increases regeneration of myofibres in *mdx* mice[67].

Reduction of oxygen in culture to 1% increases quiescence, decreases differentiation, and increases self-renewal of satellite cells[68, 69]. Hypoxia induces upregulation of the PAX7, and down regulation of miR-1 and miR-206 through the Notch pathway[69].

Other methods involve mimicking the satellite cell niche in order to preserve self-renewal of satellite cells *ex vivo*. The niche includes the myofibre on which satellite cells rest. This pliable surface has also been shown to retain quiescence of satellite cells[65]. Satellite cells cultured on polyethylene glycol hydrogel substrates with pliability similar to myofibres in vivo were superior in their ability to engraft into dystrophic muscle, compared to satellite cells cultured on more rigid hydrogel coating[65]. Like hypoxia, culture of satellite cells on a pliable substrate may preserve self-renewal through signalling pathways that maintain self-renewal of satellite cells in their niche.

Therapeutic Potential of miR-31

MicroRNAs

Role of microRNAs

The cells of an organism all contain the same genomic DNA, but acquire tissue identity through the selective expression of genes[70]. Cells must retain adequate levels of the proteins required to confer their cell phenotype, in response to the extracellular environment[70]. Levels of transcripts in the cell are dynamic. Despite processing steps to reinforce their stability, mRNAs have relatively short half-lives in eukaryotic cells[71]. Gene expression may be regulated at the levels of initiation of transcription; post-transcriptional modification and processing of transcripts; transport and stability of transcripts; initiation and continuation of translation; as well as transport and stability of the encoded protein[71].

Occasionally a cell invests in transcription before a protein is actually required, rather than relying on initiation of transcription which takes hours[18, 71]. One mechanism of post-transcriptional modulation of gene expression is through microRNAs. MicroRNAs are small functional RNAs that generally act as “fine-tuners” of cellular processes in homeostasis[72].

Biogenesis of microRNAs

MicroRNA expression begins with transcription of miRNA genes into a hairpin structure flanked by single stranded regions, called the primary miRNA (pri-miRNA) (Figure 4)[73]. The pri-miRNA is cleaved co-transcriptionally within the stem region by the nuclear microprocessor complex, which includes the exonuclease Drosha and its partner DiGeorge critical region 8 [73]. This yields the precursor miRNA (pre-miRNA), a ~70nt stem loop structure [74]. A complex formed of Exportin-5 and Ran-guanosine triphosphate facilitates export of pre-miRNAs from the nucleus [73].

In the cytoplasm, the pre-miR is met with the RISC loading complex (RLC) [73]. Components of the RLC include the RNase Dicer, the catalytic component Argonaute-2 (Ago2), the Tar RNA binding protein (TRBP) and protein activator of PKR (PACT) [73]. Dicer trims away the loop region to give the mature miRNA duplex, which is approximately 22 nucleotides in length[73]. Dicer and TRBP then dissociate from the RLC to leave the RNA-induced silencing complex (RISC) [73]. As a part of the RNA-induced silencing complex (RISC), Ago2 cleaves the passenger strand while a helicase component of RISC unwinds it from the function microRNA for degradation[73].

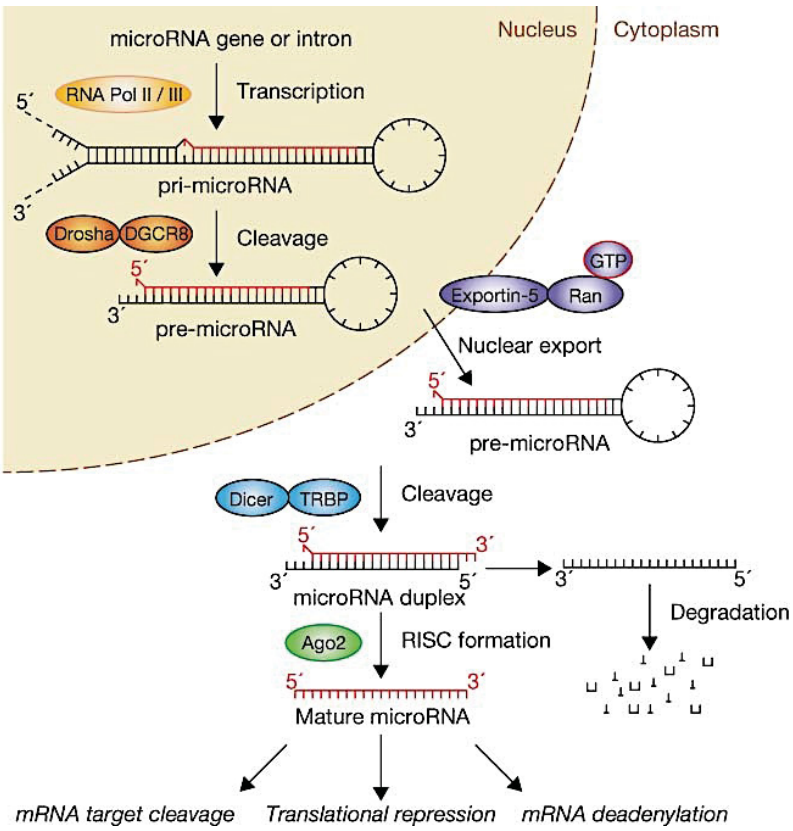

Figure 3: MicroRNA biogenesis and function. Image from Winter, J. et al.; Nat Cell Biol, 2009[73].

Targeting of messenger RNAs

In animals, microRNAs bind to targets based on partial complementarity between the approximately 22-nucleotide miRNA and the miRNA recognition element, typically within the 3' untranslated region, of the mRNA[75]. Various algorithms are used for *in silico* prediction of miRNA target sites[75]. Effective binding of miRNAs *in vivo* is mainly predicted by complementarity within the seed region, from nucleotide 2 to 7; however, this is neither necessary nor sufficient in identifying real miRNA targets[75].

Post-transcriptional control of gene expression includes sequestration of translatable mRNAs. Several types of RNA granules found in the cytoplasm contain mRNAs, which can re-associate with ribosomes for translation upon changes in the cellular environment[71]. MiRNA-mediated translational silencing has been shown to coincide with mRNA trafficking to RNA granules[71].

Importance of microRNAs in Myogenesis

In the absence of microRNA biogenesis, perinatal death ensues due to skeletal muscle hypoplasia[76]. MyomiRs are a group of skeletal muscle specific microRNAs that play a role in the equilibrium between proliferation and differentiation of myoblasts[76]. Disrupted expression of miRNAs has been observed in a number of muscular disorders, including DMD[38]. Nitric oxide (NO) signalling in skeletal muscle allows nitrosylation of histone deacetylase 2 (HDAC2)[76]. HDAC2 is involved chromatin remodelling at the promoters of miR-1 and miR-29[76]. MiR-206 represses Pax7[38], and miR-27 represses Pax3[77].

The MRFs act as transcription factors in the biogenesis of microRNA expression in myoblasts. Myogenin and MyoD bind upstream to miR-1-1, miR-1-2, miR-133a-1, miR-133a-2 and miR-206, which are all specifically induced during myogenesis and appear to have a role in differentiation[78]. Myogenin and MyoD also bind upstream of miR-100, miR-191, miR-138-2 and miR-22[78]. MiR-30a and miR-206 have been implicated in a regulatory feedback loop; in which MRFs induce their expression, and they target and remove Snai1 and Snai2 transcription factors, which block the action of MYOD in myogenesis[17]. Targets of miR-1 and miR-133 include the Notch pathway and BMP2 pathways, and miR-1 has been implicated in the down-regulation of HDAC4, which negatively regulates myogenesis[78]. MiR-1 and miR-133 repress transcription of myoblast-associated genes in favour of genes involved in the formation of myotubes[78].

MicroRNA-31

Expression of microRNA-31

MicroRNA-31 (miR-31) has been identified as the most upregulated miRNA in skeletal muscle tissue from DMD patients[79], as well as *mdx* mice[80]. Paradoxically, miR-31 is found to be present in quiescent satellite cells[18]. Upregulation of miR-31 in dystrophic muscle is likely due to both the increased activation and proliferation of satellite cells in response to chronic injury, and the impaired differentiation potential of dystrophic myoblasts[81].

MicroRNA-31 targets Myf5

As previously mentioned, quiescent satellite cells express the *Myf5* transcript, which is retained in mRNP granules until they are activated from quiescence[18, 42]. Likewise, miR-31 is found in granular foci of quiescent satellite cells. MiR-31 has a target site on the 3' untranslated region (UTR) of the *Myf5* transcript (Figure 4A) [18, 82]. Lipid-mediated transfection of satellite cells with miR-31 has been shown to significantly increase levels of miR-31, decrease expression of MYF5, and delay the later stages of the myogenic program (Figure 4B). *In situ* hybridization, gradient centrifugation, and co-immunoprecipitation experiments have indicated that miR-31 and *Myf5* are found in mRNP granules in quiescence satellite cells[18]. Repression of translation has been validated *in vitro* by luciferase assay in HEK293 cells, as well as *ex vivo* by polysome experiments, in which miR-31 and *Myf5* are found within the light fraction from quiescent satellite cells[18]. This is evidence that miR-31 retains *Myf5* in messenger ribonucleoprotein particles (mRNP) for later expression of MYF5 upon entry into the myogenic program[18].

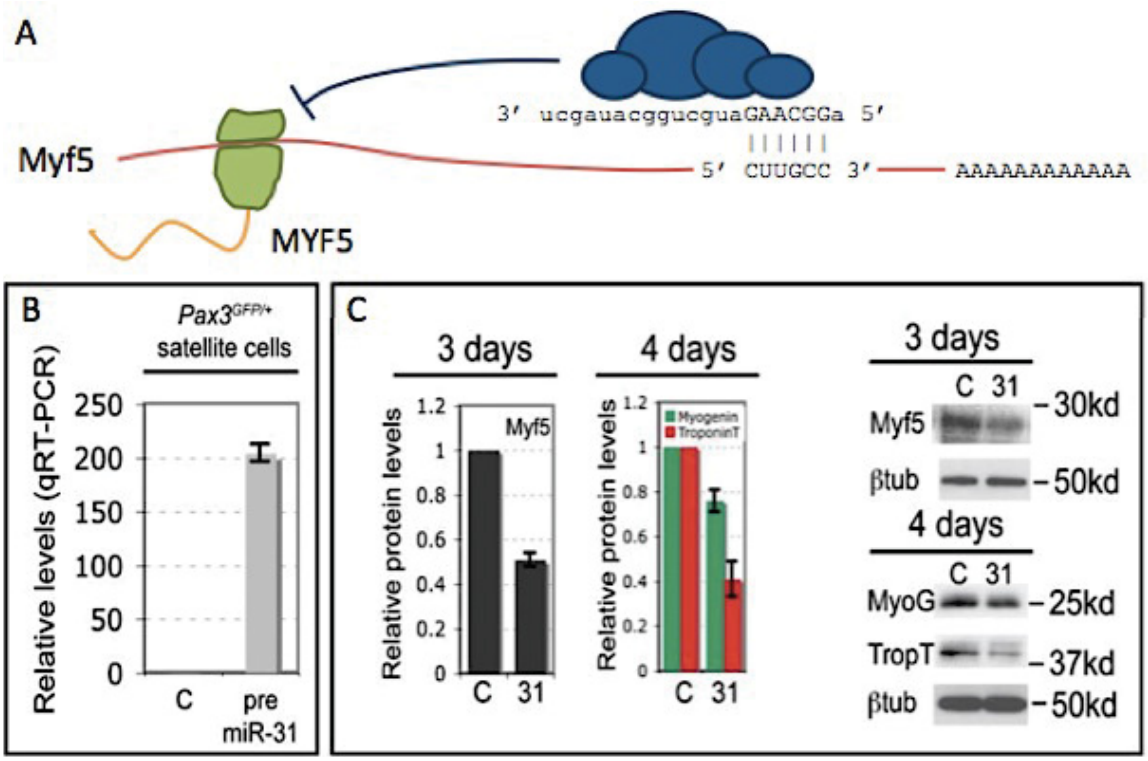

Figure 5: Lipid-mediated transfection with miR-31 decreases MYF5 expression and progression through the myogenic program. A) MiR-31-RISC binds to the 3' UTR of the *Myf5* transcript to inhibit translation. The complementary region of the *Myf5* transcript is shown below the seed region of the mature miR-31 sequence. B) Lipid-mediated transfection with pre-miR-31 effectively increases levels of miR-31 in satellite cells. C) Pre-miR-31 treatment reduces MYF5 after 3 days in culture, and reduces levels of proteins involved in forming new muscle fibres after 4 days in culture. Panels B and C obtained from Crist, C.G., Montarras, D. & Buckingham, M.; Cell Stem Cell, 2012.

MicroRNA-31 targets Fxr1

The fragile X related (FXR) family of ribonucleic acid (RNA)-binding proteins includes FXR1P and FXR2P, which are paralogs of fragile X mental retardation protein (FMRP)[83]. FXR proteins are associated with ribosomes in messenger ribonuclear particles (mRNPs)[84]. They have been implicated in intracellular transport and translational inhibition of target messenger ribonucleic acids (mRNAs)[84]. Like FMRP, FXR1P and FXR2P bind RNAs via a K protein homology 2 domain[83]. Alternative splicing results in the presence of several isoforms of FXR1P[84]. The 70, 74, 78 and 80 kilodalton (kDa) isoforms are widely expresses in various cell lines and tissue types, but are absent in the skeletal muscle, where 82 and 84 kDa long isoforms are uniquely expressed[85].

The short isoforms are expressed in myoblasts, but give way to the longer muscle specific isoforms as differentiation to myotubes occurs[85]. The 84 kDa isoform of FXR1P has high affinity for mRNAs that contain a G quartet[84]. In fascioscapulohumoral muscular dystrophy (FSHD) patients, expression of skeletal muscle specific isoforms of FXR1P is decreased[86, 87]. This is caused by reduced stability of *Fxr1* mRNA[86]. *Fxr1*-null mice have distorted skeletal muscle structure[84]. Morpholino knockdown of *FXR1* in *Xenopus* leads to impaired somite formation[85]. Similarly, *fxr1* knockdown causes abnormal myotome formation in zebrafish[84]. The importance of *Fxr1* in muscle development supports a relationship between decreased FXR1P expression and the FSHD phenotype.

In zebrafish, fxr1 knockdown results in shortening of the stripe expression pattern of MYOD in the embryo[84]. In Xenopus, morpholino knockdown of FXR1 results in a diffused pattern of expression in place of normal MYOD stripe formation[85]. These experiments support a role for Fxr1 in the localization or regulation of translation of MyoD. Knockdown of Fxr1 has been shown to ablate differentiation due to impaired MYOD expression[85]. MicroRNAs play a role in many muscular dystrophy disorders, which may include FSHD[88]. MiR-31 has a predicted target site on 3' UTR of fragile X-related protein 1 (*Fxr1*)[82], and could potentially mediate this deregulation. Expression of miR-31 is upregulated 1.76-fold in human FSHD myoblasts relative to normal myoblasts[89].

Thesis

Hypothesis

Transfection of satellite cells with microRNA-31 will promote self-renewal of satellite cells *ex vivo*, and engraftment *in vivo* following transplantation.

Research Aims

Effects of microRNA-31 on Self-Renewal of Satellite Cells

MicroRNA-31 is abundant in quiescent satellite cells capable of self-renewal[18]. In culture, miR-31 expression and the ability to self-renew is gradually lost as satellite cells differentiate[68, 81]. Transfection of satellite cells with miR-31 is known to delay expression of MYF5 and the myogenic regulatory factors involved in the later stages of

myogenic differentiation[18]. Exogenous expression of miR-31 is expected to retain self-renewing PAX7+/MYOD- satellite cells for longer in culture. This will be assessed by immunolabeling of myofibres and satellite cells to detect PAX7 and MYOD expression.

Effects of microRNA-31 on FXR1P Expression in Satellite Cells

The FXR1P RNA-binding protein is a potential mediator of an effect of miR-31 on MYOD expression. Since miR-31 has a target site on 3' UTR of fragile X-related protein 1 (*Fxr1*)[82], it is predicted that expression of FXR1P in satellite cells would be decreased following transfection with miR-31. This relationship is tested by luciferase assay to detect the effect of miR-31 on expression of a reporter plasmid containing the 3'UTR of Fxr1, and by western blot with lysate from miR-31 and control transfected satellite cells.

Effects of microRNA-31 on Proliferation of Satellite Cells

In addition to an increase in self-renewal, *ex-vivo* expansion of satellite cells would be beneficial to their use in cell therapy. Proliferation and cell cycle progression of miR-31 transfected satellite cells are assessed to determine whether miR-31 affects these variables.

Effects of microRNA-31 on Engraftment of Satellite Cells

Increased self-renewal of satellite cells in culture results in improved contribution to engraftment following transplantation[65, 66]. Engraftment efficiency of satellite cells will be determined by transplantation of miR-31 transfected satellite cells and myofibres into dystrophic mice. *In vivo* bioluminescence imaging will be used to assess expansion of transplanted satellite cells. Immunolabeling of cryosections from host muscle tissue will be done to detect the presence of donor-derived satellite cells capable of self-renewal.

Materials and Methods

Primary Culture

Myofibres

Collection of Myofibres

Single myofibres were collected from the *extensor digitorum longus* (EDL) muscle of the mouse hindlimb in accordance with the literature[90]. Euthanized mice were pinned to a dissection board in a prone position, and the skin over the hindlimb was carefully dissected away. The *tibialis anterior* (TA) muscle was removed at the distal tendon, carefully lifting it away from the underlying muscle, then cutting across at the proximal end. The EDL muscle was collected by cutting its distal tendon, gently lifting it from the underlying muscle, and then cutting at the proximal tendon. The EDL was incubated in 0.2% collagenase in DMEM at 37°C for 50 minutes. Digested EDL muscles were collected using a wide bore flame-polished Pasteur pipette, and deposited into DMEM-containing wells of a 6 well tissue culture plate. The EDL was triturated up and down to liberate single myofibres.

Culture of Myofibres

Single myofibres were collected using a cut 1000ul pipette tip, pre-charged with satellite cell culture medium, and transferred to new 2ml microcentrifuge tubes. Fibres were cultured in suspension with satellite cell culture medium in the microcentrifuge tubes with needle-punched holes in the lid. Since culture of single myofibres on gelatin-coated plates causes delamination and activation of satellite cells to form myocolonies, myofibres remained in suspension for the duration of tissue culture.

Pax3GFP/+ satellite cells

$Pax3^{GFP/+}$ mice

$Pax3^{GFP/+}$ mice allow direct isolation of satellite cells by flow cytometry for green fluorescent protein (GFP). The gene for enhanced GFP has been inserted into one allele of the *Pax3* gene, replacing the coding sequence of exon 1[91]. *$Pax3^{GFP/+}$* mice are bred over a

C57 black 6 background. A white splotch in the fur of the abdomen identifies *Pax3*$^{GFP/+}$ mice. Immunohistochemistry has demonstrated the presence of GFP+ nuclei in the satellite cell niche between the basal lamina and the sarcolemma, marked by laminin and dystrophin respectively, in diaphragm and abdominal muscle of *Pax3*$^{GFP/+}$ mice[92].

Collection of Satellite Cells by Flow Cytometry

Abdomen and diaphragm muscles were collected approximately 6-week-old *Pax3*$^{GFP/+}$ mice. Blood and debris were removed with curved forceps, and then micro-scissors were used to chop the muscle into coarse slurry. A series of enzymatic digests were performed with trypsin collagenase media (0.25% Collagenase D + 0.25% Trypsin in F12 media, without penicillin-streptomycin (-P/S)). The cell suspension was transferred into FBS and stored on ice after each digest to inactivate the trypsin and collagenase. The suspension was filtered through 80-micron cloth, pelleted, and re-suspended in 2ml of collection media (F12 media 10% FBS -P/S). The concentrated suspension was filtered again through 80-micron cloth, and then through a 35μm cell strainer cap into a polypropylene tube. Propidium iodide (PI) was added at a final concentration of 1μl per ml to stain dead cells. GFP+, PI- cells were isolated by flow cytometry. Forward and side scatter are used to screen for small non-granular cells, enriching for satellite cells [93].

Culture of Satellite Cells

Satellite cells were cultured for immunocytochemistry and various assays. Cells were seeded at a density of 7,500 cells per 35mm plate. Plates were coated with 0.1% gelatin[94]. Culture medium was composed of 40% F12 (Gibco), 40% DMEM (Gibco), 20% FBS, plus 1:25 Ultroser G (Pall) supplement +P/S. Ultroser G is an artificial supplement composed of growth factors including fibroblast growth factor, insulin-like growth factor, and epidermal growth factor, used to promote proliferation of satellite cells in culture[95].

Lipid Mediated Transfection

Synthetic microRNAs

Synthetic microRNAs

MicroRNA-31 was exogenously expressed by delivery of a synthetic mimic of endogenous miRNA-31. Initial experiments were conducted with Pre-miR™ miRNA Precursor (Ambion®), a small double-stranded RNA molecule chemically modified to improve stability. Later experiments were performed with the next generation of synthetic miRNA: mirVana™ miRNA Mimic (Ambion®).

Control Oligonucleotides

For experiments conducted with Pre-miR™ miRNA Precursor, Pre-miR™ miRNA Precursors Negative Control #1 (Ambion®) was used to treat negative control satellite cells and myofibres. mirVana™ miRNA Mimic Negative Control #1 (Ambion®) was used to treat negative control satellite cells in experiments using mirVana™ miRNA Mimic.

Lipid Transfection

Lipofectamine® RNAiMAX (Life Technologies) was used for lipid-mediated transfection of satellite cells. Human embryonic kidney 293 (HEK 293) cells were co-transfected with microRNA mimics and constructs using Lipofectamine® 2000 (Life Technologies). Lipofectamine was incubated in Opti-MEM for 5 minutes at room temperature[96]. The microRNA or negative control mimic was meanwhile diluted in OptiMEM, then added to the Lipofectamine mix and incubated for 20 minutes at room temperature[96].

Freshly isolated satellite cells were transfected for 4 hours on ice for engraftment experiments. Satellite cells were suspended in 1.5mL of satellite cell culture media -P/S per 15,000 cells. Each transfection reaction received 1.1µl of RNA and 4.5µl of Lipofectamine, both diluted in 100µl OptiMEM, per 15,000 cells.

For *in vitro* assays, satellite cells were incubated with lipid-mediated transfection reagents and miRNA mimics overnight to maximize transfection efficiency. Each 35mm

plate received 1.5µl of RNA and 5,625µl of Lipofectamine, both diluted in 100µl OptiMEM. Transfection mix was added dropwise.

Verifying Transfection Efficiency

BLOCK-iT Control

Efficiency of lipid-mediated transfection was tested by 4-hour transfection with the BLOCK-iT™ Alexa Fluor® Red Fluorescent Control on ice. At day 1 in culture, once satellite cells had adhered to tissue culture plates, live microscopy was performed.

qRT-PCR for microRNA-31

Quantitative polymerase chain reaction (qPCR) by was used to compare miR-31 levels in miR-31 (mirVANA™) and control transfected satellite cells. First, total RNA including small RNAs was isolated from satellite cells using the miRNeasy kit (Qiagen). cDNA was produced by RT-PCR. The miRCURY locked nucleic acid (LNA)™ (Exiqon) kit was used for qPCR. The kit uses ExiLENT SYBR® Green master mix. MicroRNA LNA™ PCR primer sets (Exiqon) were obtained for mouse miR-31 and U6 splicesomal RNA. Locked nucleic acids (LNA™) are RNA analogs with chemical modifications to improve stability and binding affinity. Levels of miR-31 were assessed relative to U6 spliceosomal RNA.

Fxr1 Expression and Targeting by miR-31

Cloning of *Fxr1*

3' Rapid Amplification of cDNA Ends (3' RACE)

In order to collect DNA representing the 3'UTR of Fxr1, 3' rapid amplification of cDNA ends (3' RACE) was conducted. Total RNA was collected from *Pax3*$^{GFP/+}$ satellite cells at day 3 and day 5 in culture. The SMARTer RACE cDNA Amplification kit (Clontech) was used according to the kit instructions.

Addition of Restriction Enzyme Recognition Sites

Two splice variants of the *Fxr1* transcript are expressed in mice[97]. Overhang primers were designed to target the 3' end of *Fxr1* variant 1 (*Fxr1v1*) and *Fxr1* variant 2 (*Fxr1v2*), with the addition of a XhoI restriction site. A 5' overhang primer was designed to

target both variants, and add a NotI restriction site. PCR was performed to amplify *Fxr1v1* and *Fxr1v2* flanked by NotI and XhoI restriction sites. The QIAquick Gel Extraction Kit (Qiagen) was used to collect DNA following gel electrophoresis.

Sanger Sequencing

The *Fxr1v1* and *Fxr1v2* products, as well as the pGEM®-T Easy Vector (Promega), were digested with NotI. The Rapid DNA Ligation Kit (Roche) was used to ligate the products into pGEM®-T. Successful cloning disrupts the LacZ operon, allowing screening with X-Gal coated agar plates with ampicillin. DNA was collected using the QIAprep Spin Miniprep Kit (Qiagen). Sanger sequencing was conducted by the McGill University and Génome Québec Innovation Centre, starting at the T7 and SP6 RNA Polymerase transcription initiation sites. Serial Cloner 2.1 software was used to determine that the difference between *Fxr1v1* and *Fxr1v2* is upstream of the stop codon, so the 3' UTRs are identical.

Luciferase Assay

Site Directed Mutagenesis

Site-directed mutagenesis was conducted using the QuikChange II Site-Directed Mutagenesis Kit (Stratagene). The pGEM-T® Easy Vector was used for Sanger sequencing to verify fidelity and mutagenesis.

psiCheck 2 Vector

Restriction digestion of the *Fxr1 v2* and mutagenized *Fxr1 v2* (*Fxr1 v2 mut*) constructs, as well as the psiCHECK™-2 Vector (Progema) was done with NotI and XhoI. Linear *Fxr1 v2* and *Fxr1 v2 mut* products were isolated from an agarose gel using the QIAquick Gel Extraction Kit. The Rapid Ligation Kit was used to introduce the linear DNA into psiCHECK™-2. Psi-Check-2 is a luciferase reporter vector, containing a Renilla luciferase gene immediately upstream of the insert site, and a distant Firefly luciferase gene as an internal control.

Transfection and Synchronization

HEK 293 cells were plated at 5000 cells per well in a 12 well plate. Lipofectamine® 2000 (Life Technologies) was used to co-transfect the cells with 30pmol of miR-31 or negative control miRNA mimic, and 1ug of *Fxr1v2* or *Fxr1v2 mut* plasmid DNA. After a 16-hour transfection, media was replaced with serum free media (DMEM –P/S) to serum-starve the cells for 36 hours. Finally, media with serum (DMEM + 10% FBS + P/S) was introduced to allow re-entry into the cell cycle for 18 hours.

Luciferase Assay

Luciferase assay was performed manually, in triplicate, according to the Dual-Luciferase® Reporter Assay (Promega) protocol. Measurements were taken by a GloMax® 20/20 Single Tube Luminometer. The ratio of Renilla to Firefly luciferase activity of miR-31 transfected HEK293 lysate was expressed relative negative control transfected lysate for both *Fxr1 v2* and *Fxr1 v2 mut*.

Western Blot for FXR1

Preparation of Samples

At day 4 of satellite cell culture, following overnight transfection with miR-31 or negative control (pre-miR™), cells were lysed with NP-40 lysis buffer with a protease inhibitor tablet added. A cell scraper was used to collect the lysate. Novex NuPAGE LDS Sample Buffer and Sample Reducing Agent (Life Technologies) were added prior to denaturing for 15 minutes at 70°C.

Gel Electrophoresis and Transfer

Poly-acrylamine gel electrophoresis (PAGE) and transfer were performed using NuPAGE® Novex® 10% Bis-Tris Protein Gels (Life Technologies) according to the product manual. NuPAGE® 3-morpholinopropane-1-sulfonic acid SDS Running Buffer and NuPAGE® Transfer Buffer were prepared from recipes available on the Life Technologies website. The XCell II ™ Blot Module was used for both electrophoresis and transfer. Protein was transferred to Immobilon-P Membrane (Millipore) PVDF membrane.

Western Blot

The membrane was blocked in 10% skim milk in TBST (Tris-Buffered Saline + Tween 20) for 1 hour at room temperature while shaking. The membrane was cut across at 60 kDa. Antibodies were diluted in 5ml 1% milk in TBST in a 15ml conical tube. Primary antibody dilutions were 1:1500 for goat anti-FXR1 on the top section (Santa Cruz sc-10554), and 1:1000 for mouse anti-β-tubulin on the bottom. Primary antibody incubation was done in the 15ml conical tube overnight at 4°C on a roller mixer. Secondary antibodies were used at 1:10,000, with 1-hour incubation on a roller mixer at room temperature. Multiple washes were done between steps in 0.1% milk in TBST.

Visualization and Densitometry

Amersham Enhanced Chemiluminescence Prime Western Blotting Detection Reagent (GE) was added to the membrane to produce chemiluminescence from horseradish peroxidase ligated to the secondary antibodies. The ImageQuant LAS (GE) charge-coupled device imaging system was used to detect chemiluminescence. ImageQuant software was used to standardize band signal of FXR1 to β-tubulin by densitometry.

Proliferation and Cell Cycle Profiling

Detecting Proliferation

Incorporation of EdU

When cells are exposed to 5-ethynyl-2'-deoxyuridine (EdU), it becomes incorporated in their DNA during the synthesis phase (S phase) of the cell cycle[98]. Half of the satellite cell media was removed at day 3 of satellite cell culture, and replaced with satellite cell culture media containing 2X EdU. The resultant concentration of EdU in the media was 10μM. After a 4-hour window of incubation, satellite cells were fixed.

EdU Imaging Assay

An EdU imaging assay was conducted to determine the ideal time-point for fixation of satellite cells in order to detect the effect of miR-31 on proliferation. Satellite cells were fixed at day 2, 3 and 4 following a 4-hour incubation with 10μM EdU. It was determined that a 4-hour incubation at day 3 would allow the best resolution to detect the effect of

miR-31 on proliferation of satellite cells (data not shown). The Click-iT® EdU Alexa Fluor® 594 Imaging Kit (Life Technologies) was used according to the product manual. Immunofluorescence was used to simultaneously detect PAX7 using Alexa Fluor® 488nm secondary antibody.

EdU Flow Cytometry Assay

Following overnight transfection with miR-31 or negative control miRNA mimic, satellite cells were exposed to 10 μM EdU for 4 hours at day 3 in culture. The Click-iT® EdU Alexa Fluor® 647 Flow Cytometry Assay Kit (Life Technologies) was used according to the product manual. Indirect immunofluorescence was performed to detect PAX7 using Alexa Fluor® 488nm secondary antibody.

Controls for flow cytometry analysis were done on cells transfected with negative control miRNA mimic. Controls include a sample of cells not exposed to EdU, a compensation control for EdU, an isotype control for PAX7, a compensation control for PAX7, and a secondary antibody only control for PAX7. Gates were adjusted prior to flow cytometry analysis to ensure that there was no compensation between channels.

Cell Cycle Profiling

Propidium Iodide as a Marker of DNA Content

Cell cycle analysis was conducted in conjunction with the EdU Flow Cytometry Assay. PI was added at a concentration of 1μl per ml, ten minutes prior to flow cytometry. PI has access to bind total DNA of fixed and permeabilised cells, in proportion with DNA content[99]. This allows quantification of DNA content by flow cytometry based on brightness of PI signal[99].

Cell Cycle Profile

Total DNA content was used to profile the cell population, giving a distribution of the proportion of cells in various stages of the cell cycle. The lower content peak represents cells in the gap 1 phase (G1) or quiescent (G0) phase of the cell cycle, while the higher content peak represents cells in the gap 2 phase (G2) of the cell cycle, with twice the DNA of

the G1 cells[99]. Cells with intermediate DNA content are in S phase[99], while sub-G1 data points include debris and apoptotic vesicles.

Transplantation for Engraftment

Preparation of Hosts

Anaesthesia

Gas anaesthesia was performed using isoflurane. Mice were placed in an induction chamber delivering 4% isoflurane carried on oxygen at a rate of 1 L/min. Once anaesthetised, mice were transferred to the operating table where 2-2.5% isoflurane was delivered through a nose cone. Eye lubricant ointment was applied to prevent drying during anaesthesia. Depth of anaesthesia was verified by checking for the absence of reflex movement following toe pinch. Procedures were performed over a mat circulating water warmed to 34°C. Afterwards, isoflurane was turned off and mice were allowed to awaken while receiving 100% oxygen. Upon awakening, mice were returned to their cages which were placed in an incubator at 34°C for 30 minutes for recovery.

Induction into Regeneration

Cardiotoxin was diluted in phosphate buffered saline (PBS) to a dilution of 10μM, and filter sterilized. Three days prior to transplantation of satellite cells, 40μl of cardiotoxin was injected into the right TA muscle. To relieve pain associated with cardiotoxin injection, mice received subcutaneous injections of Carprofen, a veterinary non-steroidal anti-inflammatory drug, at a dose of 5ul/gram of body weight.

Voiding the Niche

Irradiation was performed at dose of 18 Gray, 3 days prior to transplantation. Mice were anaesthetized by intraperitoneal injection of mouse anaesthesia cocktail (ketamine, xylazine, and acepromazine in sterile isotonic saline) at a dose of 0.1ml/10g body weight. They were placed on a warm water bottle to prevent hypothermia during irradiation. Radiation was delivered over a period of 5 minutes using an orthovoltage x-ray tube, operated by Dr. Alasdair Syme (Medical Physics, Jewish General Hospital). Radiation was

directed specifically towards the right hindlimb of each mouse. After the procedure, mice received 1ml of sterile 0.9% sodium chloride (NaCl) subcutaneously for rehydration.

Immunosuppression to Prevent Rejection

Host mice were immunosuppressed by surgical implantation of osmotic pumps delivering the drug FK-506[100]. FK-506 (Cedarlane, #F-4900) was diluted in 70% ethanol to a concentration of 8.3µg/µl, and filter sterilized. A blunt tipped needed was used to fill each pump with 200µl of the FK-506 solution. The pumps were equilibrated in sterile 0.9% NaCl at 37°C overnight in order to initiate diffusion of FK-506 by osmosis at a rate of 0.25µl/hour. Mice were anaesthetized with isoflurane, and an electric shaver was used to remove fur from the ankle of the right hindlimb to the ribcage. A small incision was made on the back, above the right hindlimb. Round-tipped scissors were used to open a subcutaneous pocket towards to scapulae and away from the spinal column. A drop of lidocaine was applied by syringe into the subcutaneous space for local analgesia. The incision was lifted and the pump was inserted into the pocket, and then topical antibiotic ointment was applied along the incision line. Several suture clips were applied to close the incision. A dose of Carprofen was given subcutaneously following osmotic pump implantation, as well as 24 and 48 hours afterward.

Transplantation of Myofibres

Preparation of Myofibres

Transplantation of myofibres collected from EDL muscle of $Myf5^{nLacZ}$ mice was conducted based on a protocol published by Boldrin and Morgan, 2013[101]. Satellite cells that have activated the Myf5 transcript express the β-galactosidase enzyme. Hydrolysis of 5-bromo-4-chloro-3-indolyl-β-D-galactopyranoside (X-Gal) solution indicates the presence of donor-derived satellite cells. Fibres were freshly isolated immediately prior to transplantation to preserve self-renewal of myofibre-associated satellite cells. Fibres were collected with a glass-polished Pasteur pipette and transferred to a tissue culture plate containing DMEM + 10% FBS. Single myofibres were aspirated along with 5µl of medium using autoclaved 10µl PCR pipettes (Drummond) with a stainless steel plunger.

Transplantation of Myofibres

Mice were anaesthetized by isoflurane. The right hindlimb was shaved and disinfected with ethanol followed by chlorhexidine. A sterile scalpel was used to make a small incision towards the distal end of the TA muscle. The PCR pipette loaded with a single myofibre was inserted through the incision into the TA muscle. The plunger was used to expel the myofibre as the pipette was withdrawn. Antibiotic ointment was applied to the incision before the mice were allowed to recover from anaesthesia.

Transplantation of Satellite Cells

Preparation of Satellite Cells

Satellite cell suspensions were transferred to 1.5mL microcentrifuge tubes, and spun for 20min at 600g using a refrigerated centrifuge cooled to 4°C. Satellite cell pellets were re-dissolved in medium, rather than completely aspirating the medium and risking loss of the cell pellet. Injection of satellite cells in medium has been performed previously without complications[101]. The final concentration for injection was 15,000 satellite cells per 5µl of medium.

Satellite Cell Transplantation

Transplantation of satellite cells was performed using a handmade glass needle. Glass 5µl microcapillary tubes (Drummond) were pulled over flame to produce glass needles[101], which were autoclaved prior to injection. Satellite cells were concentrated for transplantation in satellite cell media without P/S.

In Vivo Bioluminescence Imaging

Engraftment Protocol

Satellite cells were collected from *Pax3*$^{GFP/+}$ *tg(Actb-luc)* mice to allow tracking of donor cells by luciferase activity. *Foxn1*$^{nu/nu}$*-mdx* nude immunodeficient mice were irradiated 3 days prior to transplantation. 15,000 *Pax3*$^{GFP/+}$ tg(Actb-luc) satellite cells were transplanted into the right TA muscle of each mouse.

In Vivo Imaging Protocol

At days 7, 14, and 21 post engraftment, mice received 10µl/g body weight of 15mg/ml D-Luciferin by intraperitoneal injection. Based on results from a kinetic curve, imaging was done 25 minutes post injection. Mice were anaesthetized using isoflurane. Imaging was done using the IVIS Spectrum Pre-clinical *In Vivo* Imaging System (Perkin Elmer) to detect epi-luminescence. Engraftment is measured in bioluminescence, defined as photons per second within a region of interest. Background from contralateral controls was subtracted from measurements. To enable comparison of images, minimum radiance was set to 10,000 and maximum was set to 500,000 (photons/second/cm^2/steradian). Bioluminescence was graphed based on total flux, ie: the number of photons per second within a region of interest.

Tissue Collection and Cryosectioning

Preparation of Tissue Samples

Isopentane was pre-chilled in a stainless steel bowl held over liquid nitrogen in double-boiler fashion. TA muscles were collected at day 21 after satellite cell or myofibre transplant. They were mounted on cork disks using tragacanth gum. The mounted TA muscles were submerged, cork facing upwards, in the isopentane. After about 1 minute, frozen TA samples were transferred into cryogenic vials pre-chilled in liquid nitrogen. Freshly frozen samples were stored at -80°C.

For detection of GFP, muscle tissue must be pre-fixed. Following dissection, TA muscles were transferred into 15ml conical tubes containing 4ml of 0.5% paraformaldehyde (PFA) in PBS, and fixed for 2 hours at 4°C. Following fixation, the PFA solution was decanted and replaced with 4ml of 20% sucrose. Muscle samples were equilibrated in 20% sucrose at 4°C overnight. The 20% sucrose was decanted and replaced with a 50:50 mix of 20% sucrose and optimal cutting temperature compound (OCT)(Fisher). The muscle samples were picked up by the tendon and submerged in pure OCT. The samples were then placed at the bottom of aluminum foil cryo-moulds made from pen caps. The samples were covered in OCT, and forceps were used to reposition them upright by the tendon. The cryo-moulds were placed in the isopentane, and transferred to a

freezer box over dry ice once freezing was complete. Pre-fixed samples were also stored at -80°C.

Cryosectioning

Fresh frozen TA samples were mounted in OCT for cryosectioning. The OCT was applied only to the cork, not touching the frozen TA muscle. Cryosections were taken at 10µm widths. For OCT-embedded TA samples, blocks were unwrapped from the aluminum foil moulds and mounted for cryosectioning with OCT. 7µm cryosections were taken at 100µm intervals[30, 92, 102, 103]. Cryosections were collected on Superfrost™ Plus coated slides (Fisher).

Immunofluorescence

Immunofluorescence on Myofibres

Myofibres were fixed in formalin for 12 minutes at room temperature. Pre-chilled methanol was used to permeabilise myofibres for 6 minutes at -20°C. Myofibres were incubated for 5 minutes in 50mM ammonium chloride (NH_4Cl). Blocking was done in 5% HS) in PBS for 1 hour at room temperature. Blocking buffer was used to dilute primary and secondary antibodies. Antibodies were diluted in blocking buffer. Primary antibodies consisted of mouse anti-PAX7 and mouse anti-MYOD (Table 1). Primary antibody incubation was done at 4°C overnight. Secondary antibodies were Alexa Fluor® 488 anti-mouse and 594 anti- rabbit (Life Technologies) as secondary antibodies along with 4',6-diamino-2-phenylindole (DAPI) to detect DNA. Myofibres were washed multiple times between steps in PBS + 0.1% FBS. Following immunostaining, myofibres were mounted on glass slides, and coverslips were applied using mounting medium (Dako).

Immunofluorescence on Satellite Cells

Satellite cells were fixed directly on the gelatine-coated tissue culture plates using formalin. Permeabilisation was done using NH_4Cl with 0.2% Triton™. Blocking was done in 0.2% gelatin in PBS for 30 minutes at room temperature. Antibodies were diluted in blocking buffer and applied in 40µl volumes. Mouse anti-PAX7 was used along with rabbit anti-MYOD (Table 1); followed by Alexa Fluor® 488 anti-mouse and 594 anti-rabbit (Life

Technologies) as secondary antibodies along with DAPI. Primary antibody incubation was done at 4°C overnight in a humidified chamber. Secondary antibody incubation was done for 1 hour at room temperature in a humidified chamber. Multiple washes were done in PBS between steps. Coverslips were mounted onto tissue culture plates using mounting medium (Dako).

Immunofluorescence on Cryosections

Detection of PAX7

Immunofluorescence to detect PAX7 was done on freshly frozen cryosections. Slides were plunged directly into formalin for 17 minutes at room temperature. Permeabilisation was done in pre-chilled methanol for 6 minutes at -20°C. Slides were incubated in NH_4Cl for 5 minutes. Demasking with citric acid buffer was done to enable detection of PAX7. Slides were immersed in 0.01M citric acid, and maintained at around 90°C using a hot water bath, twice for 5 minutes. The cryosections were blocked in Mouse on Mouse (M.O.M.) reagent for 1 hour in a humidified chamber. Multiple washes were done in PBS between steps. Antibodies were diluted in 200µl of 2% horse serum, 2% bovine serum albumin in PBS. Mouse anti-PAX7 was used along with rabbit anti-Dystrophin (Table 1); followed by Alexa Fluor® 488 anti-mouse and 594 anti- rabbit (Life Technologies) as secondary antibodies along with DAPI. Primary antibody incubation was done at 4°C overnight in a humidified chamber. Secondary antibody incubation was done for 1 hour at room temperature in a humidified chamber. Slides were mounted using mounting medium (Dako).

Detection of GFP

Donor *Pax3*$^{GFP/+}$ satellite cells retain *Pax3* expression upon engraftment into TA muscle[62]. This allows detection of donor satellite cells by immunofluorescence for GFP on cryosections[62, 92]. Since pre-fixation of tissue is required to detect GFP, pre-fixed, OCT embedded cryosections were used. A protocol was developed to allow simultaneous detection of Pax7 and GFP. Slides were plunged into 0.1% triton + 0.1M glycine in PBS for 5 minutes to permeabilise. Blocking was done in M.O.M. solution for 1 hour in a humidified chamber. Unmasking was not performed as citric acid buffer prevents detection of GFP by immunofluorescence. PAX7 can be detected without unmasking using supernatant from

PAX7 hybridoma cells (DHSB) as primary antibody diluent solution. Rabbit anti-GFP (Table 1) was diluted in PAX7 hybridoma supernatant. Primary antibody incubation was done at 4°C overnight in a humidified chamber. Secondary antibodies consisted of Alexa Fluor® 488 anti-mouse and 594 anti- rabbit (Life Technologies) along with DAPI, diluted in 5% horse serum in PBS. Secondary antibody incubation was done for 1 hour at room temperature. Multiple washes were done in PBS between steps. Coverslips were applied using mounting medium (Dako).

4-Channel Immunofluorescence

A protocol for 4-channel immunofluorescence was developed to simultaneously detect PAX7, dystrophin, GFP, and DAPI. The protocol was identical to the protocol for detection of GFP, above, with modified antibody solutions. Rabbit anti-Dystrophin and chicken anti-GFP (Table 1) were diluted in PAX7 hybridoma supernatant. Secondary antibodies consisted of Alexa Fluor® 488 anti-mouse, 594 anti-rabbit and 647 anti-chicken (Life Technologies) as secondary antibodies along with DAPI.

Antigen	Supplier	Catalogue #	Clonality	Host	Dilution
DAPI	Waterborne	D101	N/A	N/A	1:5000
Dystrophin	Pierce	PA137587	Polyclonal	Rabbit	1:3000
GFP	Abcam	ab13970	Polyclonal	Chicken	1:500
GFP	Life Technologies	A-11122	Polyclonal	Rabbit	1:3000
Ki67	BD Pharmingen	556003	Monoclonal	Mouse	1:100
MYOD	SantaCruz	sc-304	Polyclonal	Rabbit	1:100
PAX7	DHSB	N/A	Polyclonal	Mouse	1:100

Table 1: List of antibodies used for immunofluorescence.

Statistical Analysis

Statistical analysis was performed using GraphPad Prism software. Unless otherwise indicated, t-test was used for statistical analysis. Two-tailed t-test was used when data points were matched (ie: contralateral control and treated TA). Statistical significance was assigned upon obtaining a p value of less than 0.05. Significant results were marked with a "*", while non-significant results are marked "n.s." (non-significant). Unless otherwise indicated, error bars represent standard deviation. Graphs were

assembled using Microscoft Excel, except for graphs with angled x-axis labels, which were assembled in GraphPad Prism.

Results

Effects of miR-31 on Self-Renewal

Rationale

Transfection of satellite cells with miR-31 has previously been shown to result in downregulation of MYF5 and delayed progression through the myogenic program. It was anticipated that self-renewal of satellite cells may be increased as well. Self-renewing satellite cells are PAX7+/MYOD-.

Self Renewal in Single Myofibres

In order to evaluate the effect of miR-31 on satellite cells, single EDL myofibres were transfected with miR-31 (pre-miR™) or negative control overnight. Transfection with miR-31 resulted in an average increase in the proportion of PAX7+/MYOD- satellite cells among all nuclei positive for PAX7 and/or MYOD, although this was not statistically significant (Figure 5). Removal of EDL myofibres from the *in vivo* muscle environment causes activation of satellite cells, as the proportion of PAX7+/MYOD- satellite cells decreases with each day in suspension culture. Transfection with miR-31 appears to delay this process.

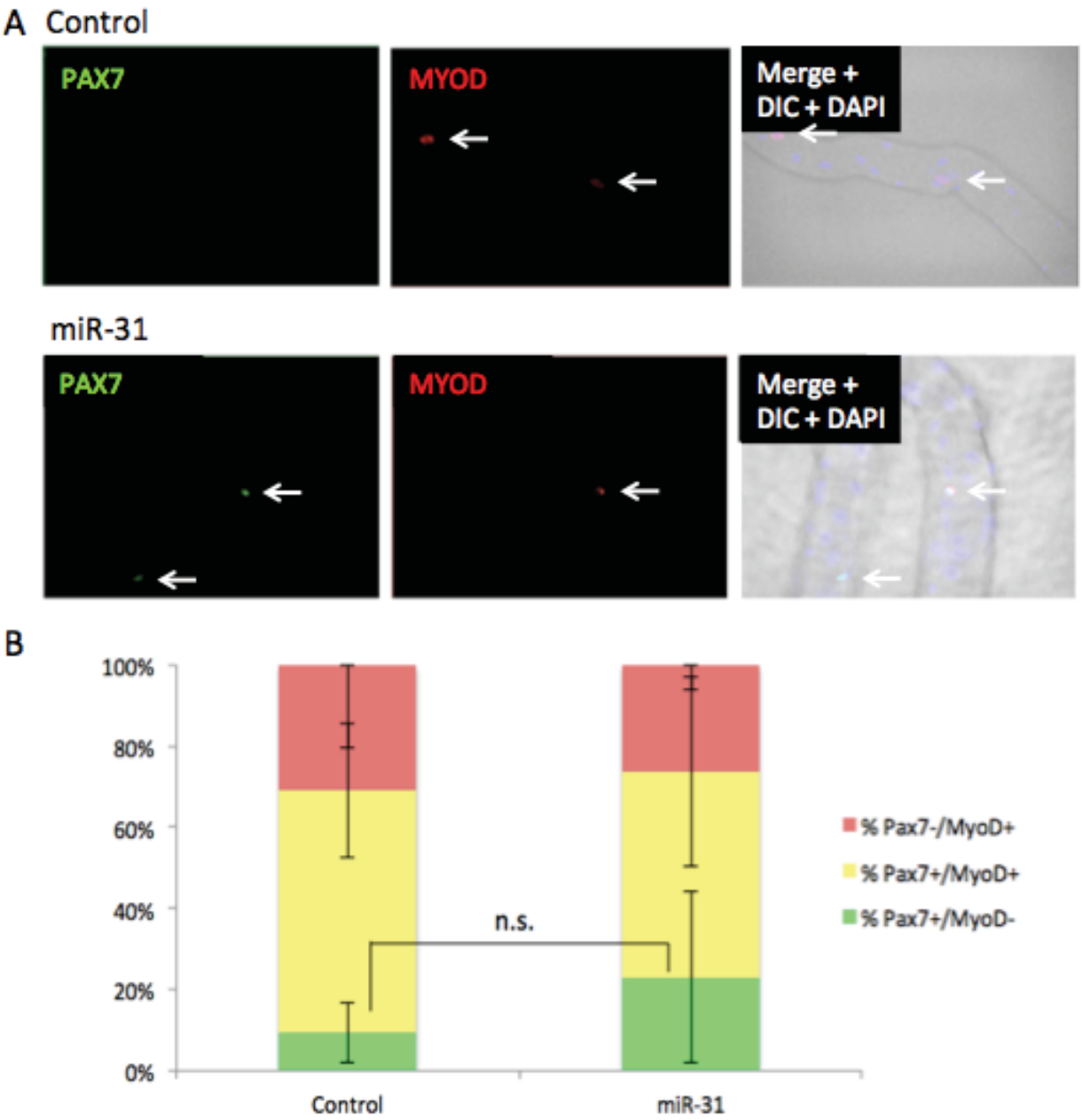

Figure 5: Effect of miR-31 on the proportion of PAX7+/MYOD- satellite cells along single EDL myofibres isolated from wildtype mice. A) Satellite cells were immunolabeled with antibodies against PAX7 (green) and MYOD (red). DAPI (blue) stained nuclei are also shown. All channels were merged over brightfield images. B) Graphic representation of results (n=150 nuclei for control, n=145 nuclei for miR-31).

Self-Renewal of Isolated Satellite Cells

Direct lipid-mediated transfection of satellite cells in culture was done to determine whether miR-31 would increase the proportion of PAX7+/MYOD- self-renewing satellite

cells in the absence of the myofibre environment. This allowed characterization of more cells, obtained by flow cytometry from *Pax3*$^{GFP/+}$ mice, in absence of the myofibre. Overnight transfection of freshly isolated satellite cells with miR-31 (pre-miR™) resulted in a significant increase in the proportion of PAX7+/MYOD- satellite cells at day 3 in culture (Figure 6). This supported the previous finding that miR-31 delays entry into the myogenic program[18]. The results matched what was detected along single EDL myofibres, with an additional decrease in PAX7-/MYOD+ satellite cells.

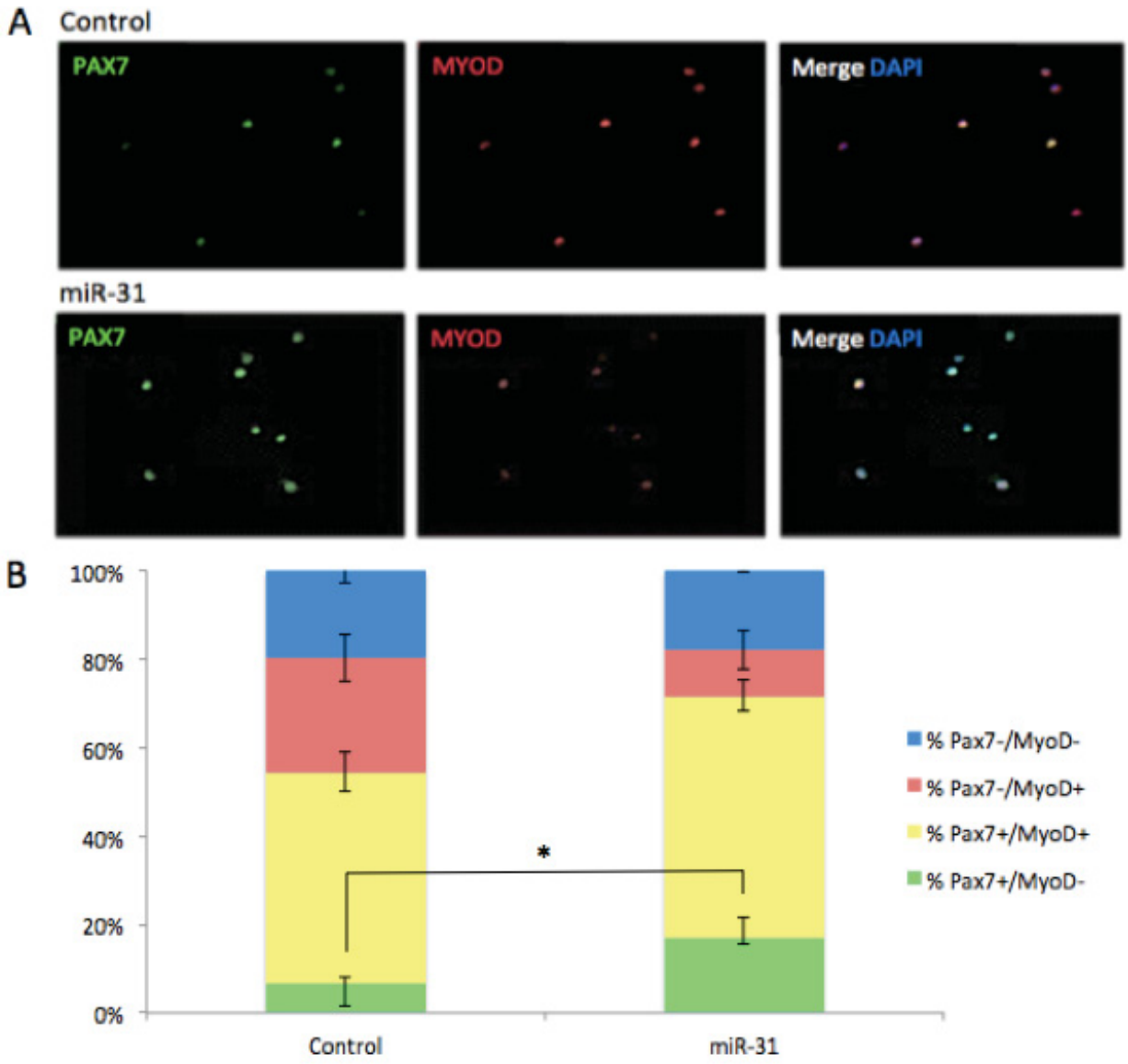

Figure 6: MiR-31 increases the proportion of PAX7+/MYOD- satellite cells in culture. A) Satellite cells were immunolabeled with antibodies against PAX7 (green) and MYOD (red), merged over DAPI (blue) stained nuclei. B) Graphic representation of results. Blinded characterization of cell phenotypes (n=200 nuclei per condition, in triplicate; p=0.007).

Effects of miR-31 on FXR1P Expression

Rationale

Since there is no predicted target site for miR-31 on the 3'UTR of the *MyoD* transcript, effects of miR-31 on increasing PAX7+/MYOD- satellite cells are due to indirect effects on MYOD. A potential explanation is targeting of the *Fxr1* transcript by miR-31.

FXR1P is an RNA binding protein known to regulate MYOD expression. High levels of miR-31 in FSHD myoblasts could lead to their decreased levels of skeletal muscle specific FXR1P isoforms.

Expression of Fxr1 transcript

3'RACE for *Fxr1* was conducted on day 3 and day 5 of satellite cell culture. When the products were run on an agarose gel, two products were obtained at day 3 (Figure 7). Sanger sequencing revealed that one product was missing exon 16, upstream of the stop codon. The 3'UTR region of both products aligned perfectly to *Fxr1* variant 2 (*Fxr1 v2*), and contained the 6nt target site for miR-31.

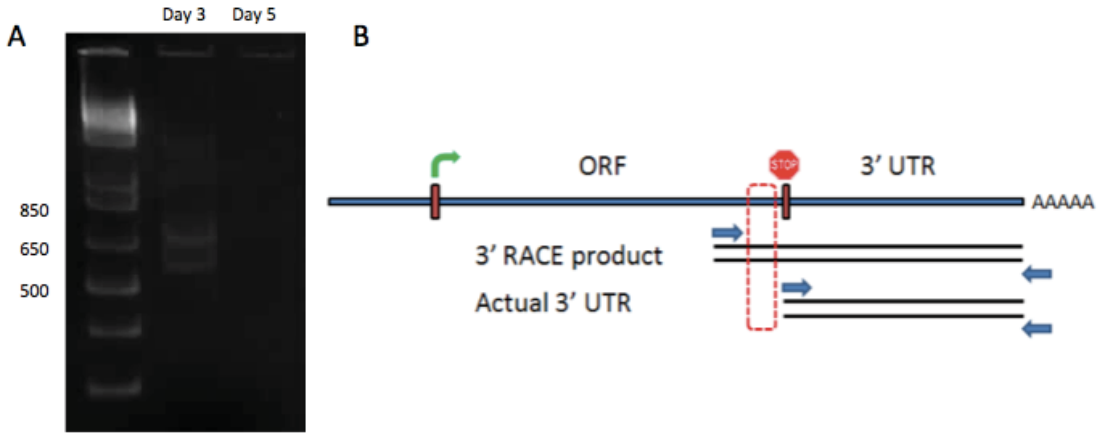

Figure 7: Products of 3' RACE for *Fxr1* expression in satellite cells. A) Two bands were seen at *Fxr1* in SCs at day 3 in culture, while no DNA bands were seen at day 5 in culture. B) Sanger sequenced revealed that the difference in was upstream of the stop codon; the two 3'UTR sequences were identical.

Targeting of Fxr1 by miR-31 *In Vitro*

A luciferase assay was conducted to determine whether miR-31 was capable of inhibiting translation of *Fxr1 v2* in vitro. Serum starved HEK 293 cells were co-transfected with *Fxr1 v2* and miR-31 or negative control (pre-miR™). Expression of FXR1P was detected by expression of Renilla luciferase, standardized to Firefly luciferase expression. In the presence of *Fxr1 v2*, exposure to miR-31 significantly reduced the Renilla:Firefly luciferase ratio by approximately 34% compared to the control (Figure 8). This decrease was rescued by site-directed mutagenesis removing the miR-31 target site on *Fxr1 v2*.

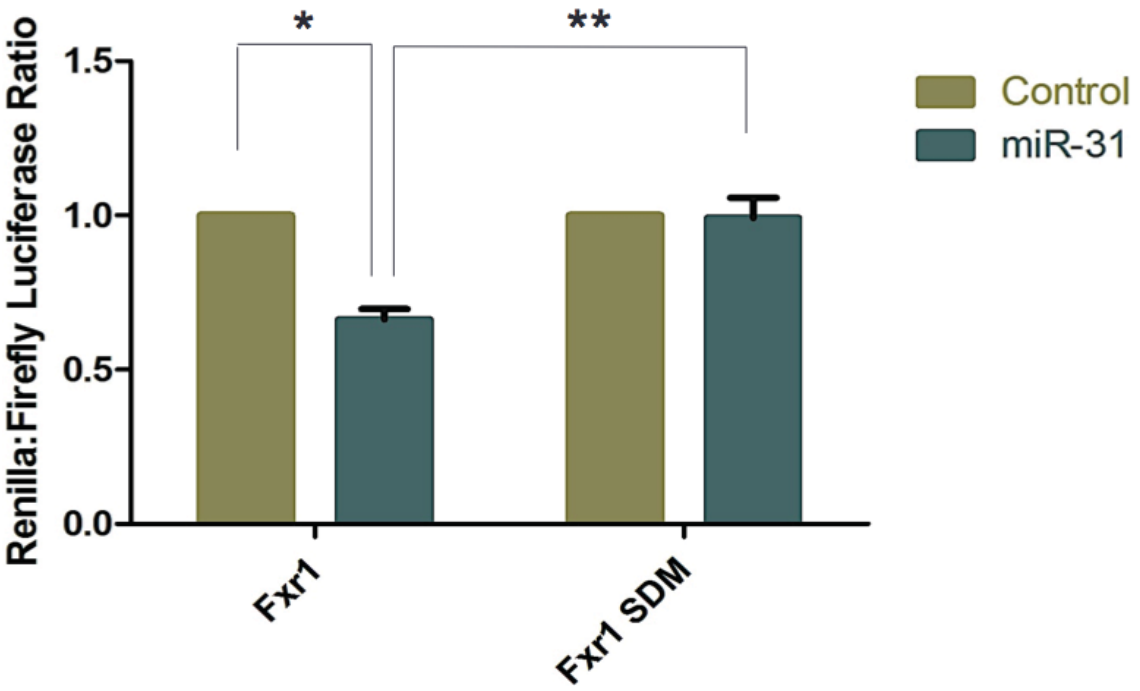

Figure 8: MiR-31 decreases FXR1 expression *in vitro* by luciferase reporter assay. Renilla:Firefly luciferase expression was expressed as a ratio of miR-31 to control. Three experimental replicas were done. Error bars are standard error of the mean. Significance based on two-way ANOVA, * p = 0.0015, ** p = 0.0019.

Western Blot to Detect Effect of miR-31 on Satellite Cells

In order to determine whether miR-31 is also capable of reducing levels of FXR1P in satellite cell culture, western blot was performed. Detection of FXR1P proved challenging. In order to maximize protein concentration, satellite cells were seeded at 10,000 cells per plate, and lysate was collected at day 4 in culture. Concentration of primary antibody was reduced to 1:15,000 to increase the contrast between FXR1P and background staining. Fxr1 is alternatively spliced to produce seven different isoforms[86]. The widely expressed ~78 kDa isoform was reduced by miR-31 transfection (Figure 9). Importantly, the ~84 kDa skeletal muscle specific isoform was undetectable in miR-31 transfected cell lysate. The upper band at ~94 kDa represents FXR2P, and is the result of a cross-reaction of the FXR1P antibody[86, 104]. The putative identity of each band would need to be confirmed by siRNA experiments.

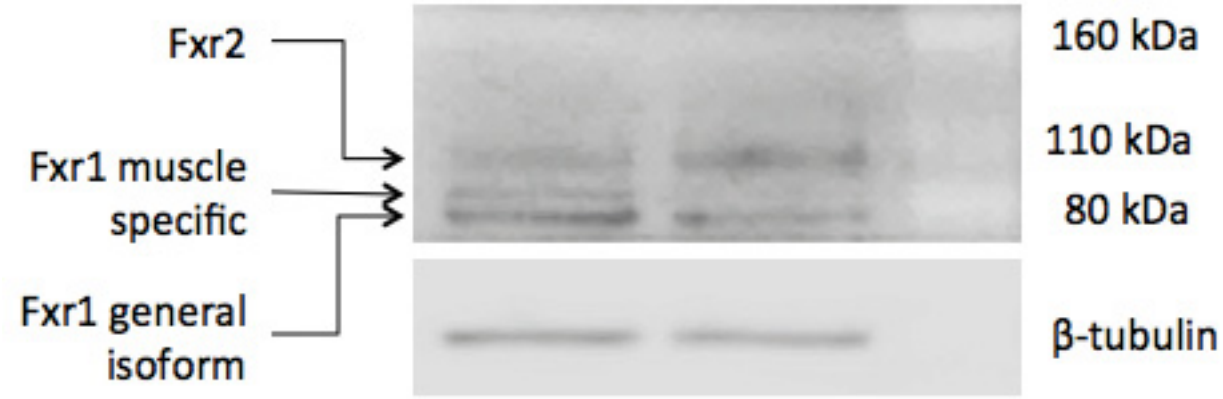

Figure 9: Western blot to detect the effect of miR-31 on FXR1P expression in satellite cells. A) Image of western blot, containing protein markers on either side. Arrows indicate putative indentity of proteins, based on molecular size. A band for β-tubulin was detected at ~55 kDa as predicted.

Effects of miR-31 on Proliferation, Cell Cycle and Viability

Rationale

It was noted that at day 3 in culture, cell colonies arising from miR-31 transfected satellite cells appeared to be denser (Figure 10). Plates transfected with miR-31 appeared to contain more doublets of nuclei, suggesting recent cytokinesis. This suggests that miR-31 may increase proliferation of satellite cells and/or their differentiating progeny.

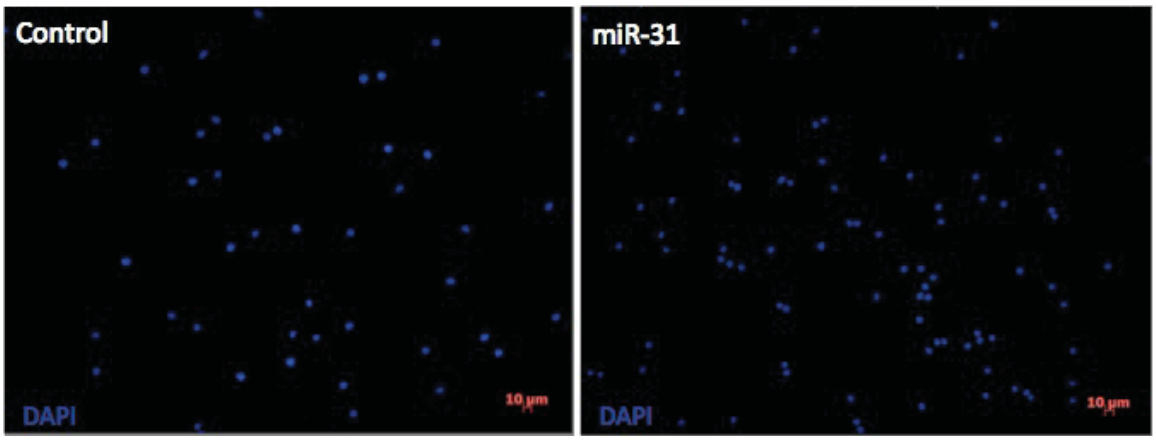

Figure 10: Colony density is increased in miR-31 transfected satellite cells. Images are representative of densest colonies from miR-31 and control transfected plates at day 3 in culture. Nuclei are stained with DAPI (blue).

Proliferation by EdU Incorporation

Incorporation of EdU over a 4-hour exposure period allowed detection of the proportion of cells that had undergone proliferation within that period of time. At day 3 in culture, the percentage of PAX7+/EdU- cells is not significantly increased (Figure 11).

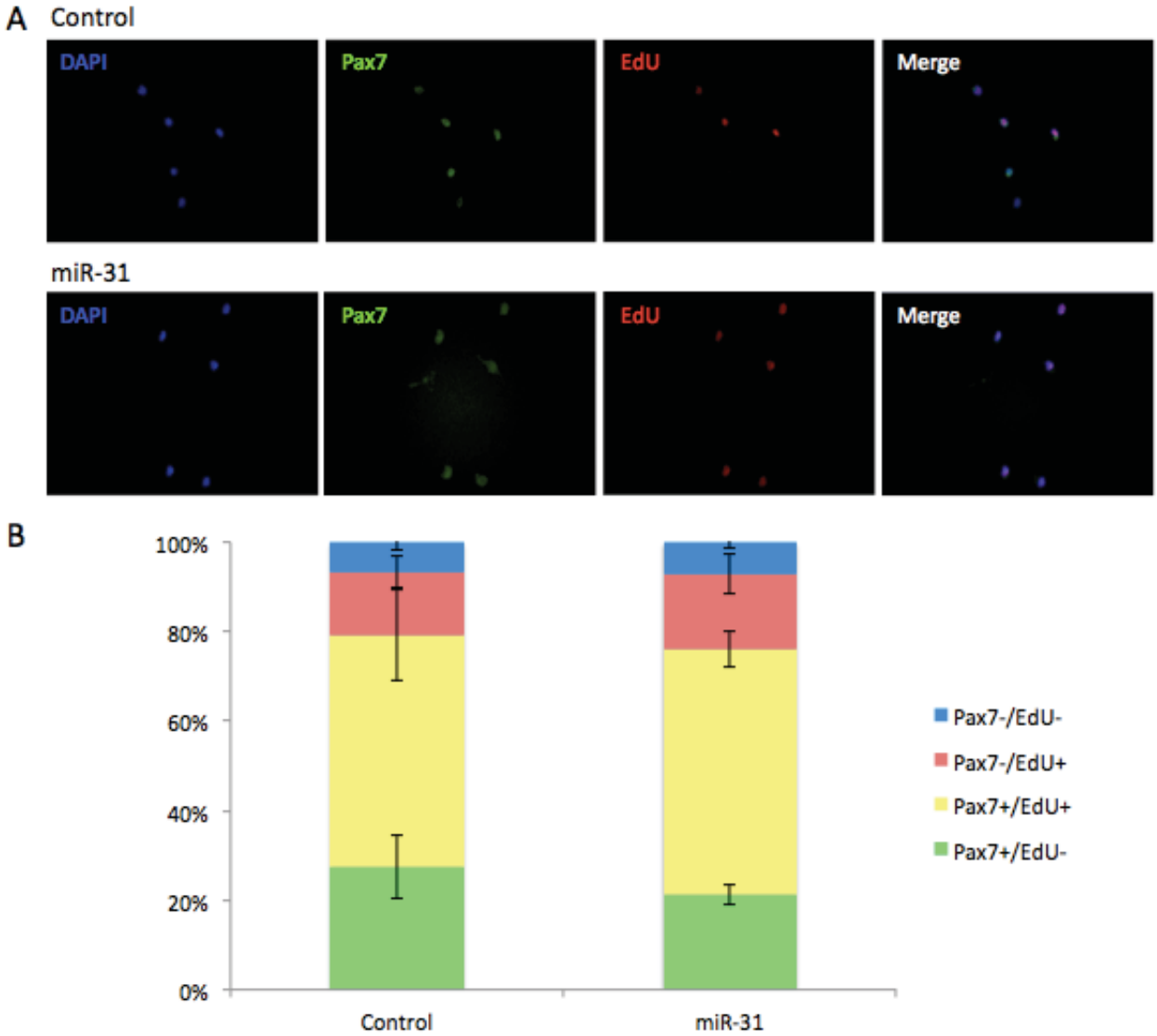

Figure 11: EdU proliferation imaging assay on satellite cells at day 3 in culture. A) Cells were immunolabeled with an antibody against PAX7 (green), a fluorescence azide was bound to EdU (red), and these channels were merged over DAPI (blue) stained nuclei. B) Graphic representation of results. Transfection with miR-31 did not significantly alter the proportion of any of the cell phenotypes, measured by two-way t-test; n=200 nuclei per condition, in biological triplicate.

Cell Cycle and Proliferation by Flow Cytometry

The EdU incorporation assay was repeated at day 3 in culture using the flow cytometry kit. Cell cycle profiling by DNA content, measured by PI staining, suggested a slight increase in the proportion of cells in the S phase of the cell cycle (Figure 12). This could be attributed to more rapid cycling through the cell cycle, although the difference is likely too small to account for the differences seen in plates of miR-31 vs. control transfected satellite cells at day 3 in culture. There appeared to be an increase in the proportion of EdU negative cells at G2/M phase. No major difference was detected in the proportion of sub G1 data points, which include debris and apoptotic vesicles, suggesting that the rate of apoptosis is not affected by miR-31.

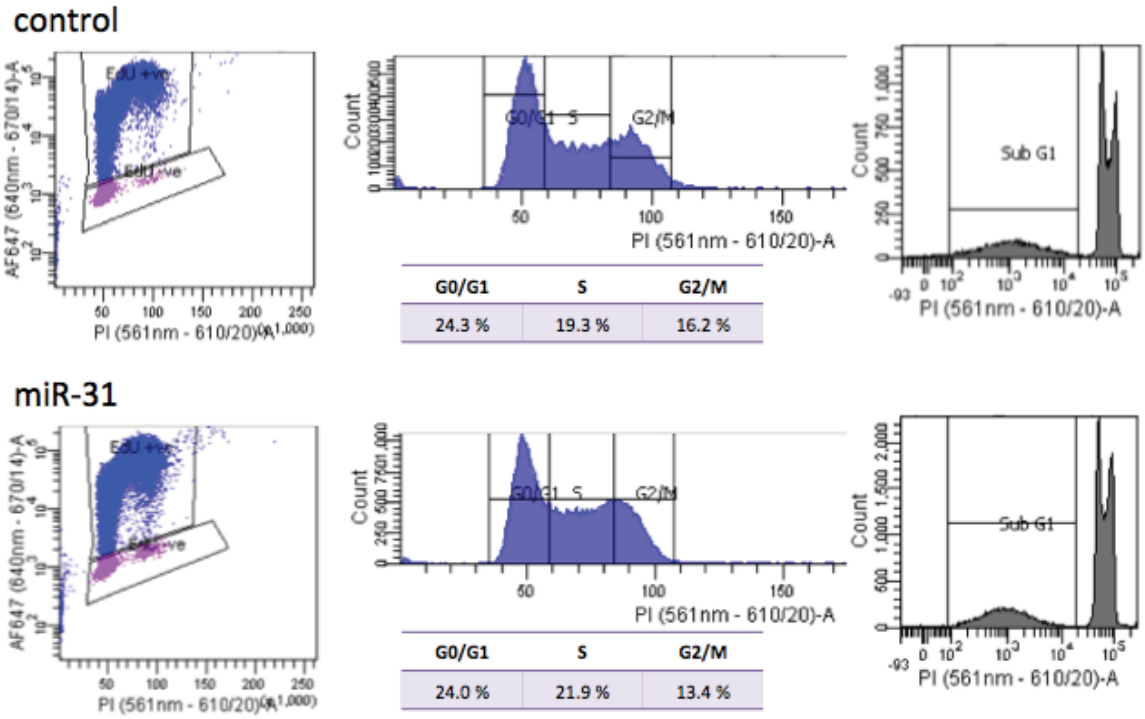

Figure 12: EdU incorporation and cell cycle profile by flow cytometry. Approximately 50,000 cells were analyzed for miR-31 transfection, and 25,000 cells for control transfection. On left, EdU signal (y-axis) was plotted against DNA content (x-axis). At centre, proportion of cells (y-axis) was plotted against DNA content (x-axis), allowing estimation of the percentage of cells in each phase of the cell cycle (below). On right, the proportion of events (y-axis) was plotted against DNA content (x-axis) to compare the proportion of sub-G1 DNA content events.

Effects of miR-31 on Engraftment

Rationale

Regardless of whether transfection of satellite cells with miR-31 is involved in *ex vivo* expansion of satellite cells, it has been shown to promote self-renewal in culture. Upon transplantation, satellite cells with enhanced self-renewal are expected to contribute better to engraftment through and repopulation of a depleted satellite cell niche.

4 Hour Transfection

In order to determine the effects of miR-31 on satellite cells, effective exogenous expression had to be achieved. Lipid-mediated transfection with synthetic miR-31 overnight has previously been shown to increase levels of miR-31 in satellite cells, and prevent the accumulation of MYF5. We hypothesized that 4-hour transient lipid-mediated transfection would also lead to overexpression of miR-31.

Assessment of transfection conditions with BLOCK-iT

To assess whether lipid-mediated transfection for 4 hours on ice permitted efficient delivery of synthetic microRNAs, a BLOCK-iT™ transfection efficiency assessment was done. Thirty GFP+ satellite cells were characterized as positive or negative for transfection with BLOCK-iT™ Alexa Fluor® Red based on emitted light in the Cy3 channel (Figure 13). Of 30 nuclei, 29 were found to be BLOCK-iT positive; transfection efficiency was found to be approximately 97%. This indicates that the transfection conditions would allow efficient delivery of synthetic miRNA mimic.

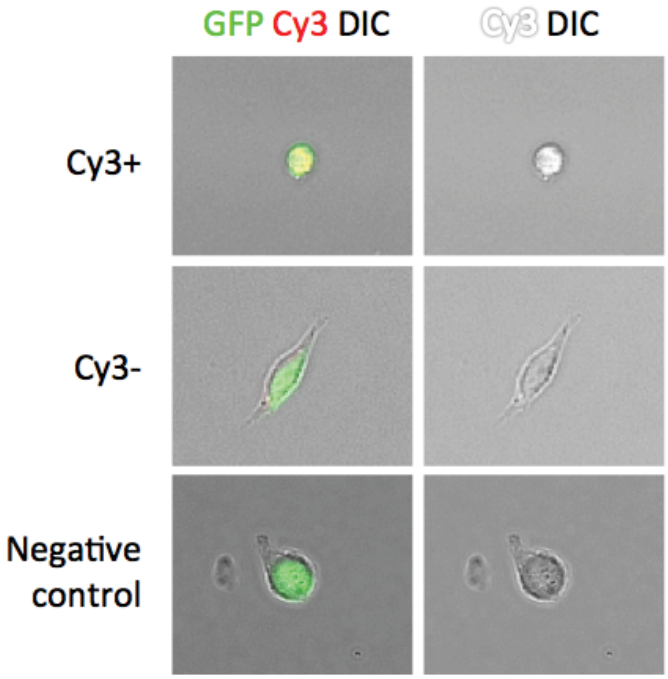

Figure 13: Testing of lipid-mediated transfection protocol with BLOCK-iT Cy3 labeled oligonucleotide. Representative images of Cy3+, Cy3-, and negative control GFP+ satellite cells. Images were taken at day 1 in culture. Cy3 staining is shown in red on the merged images with GFP, and in white over brightfield, right.

Levels of miR-31 by qPCR

With the intention of more accurately assessing the delivery of miR-31 by lipid-mediated transfection with miR-31 mimic (mirVANA™), miR-31 levels were measured by qPCR. MicroRNA was collected from miR-31 and negative control transfected cells at day 3 in culture. Relative to negative control transfected cells, miR-31 transfected cells lead to approximately a 200-fold increase in miR-31 levels, standardized to U6 spliceosomal RNA (Figure 14).

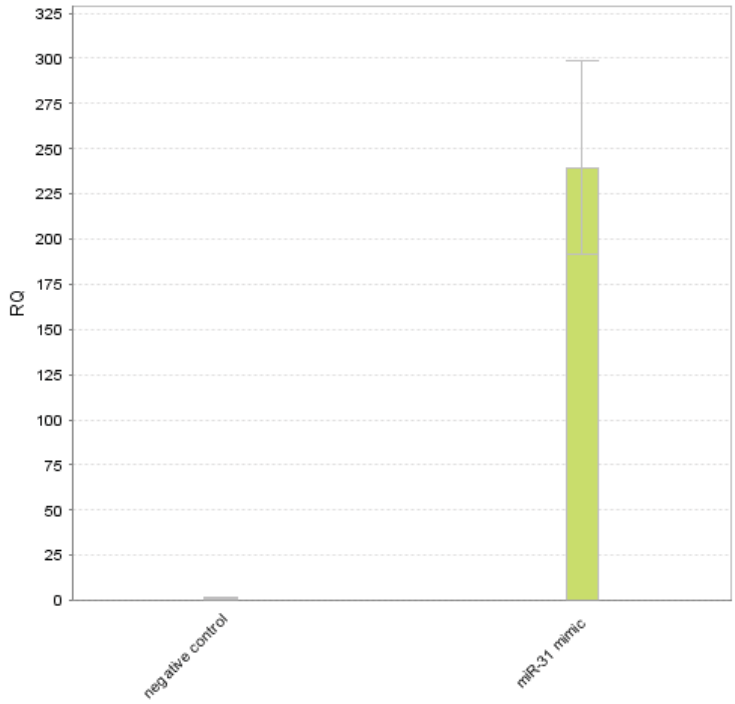

Figure 14: Transfection with miR-31 leads to a robust increase in miR-31 levels by qPCR. Expression is measured in relative quantity (RQ) indicating fold increase over negative control, relative to U6. Error bars are standard deviation (n=6).

Revertant Fibres

Mdx mice exhibit revertant fibres, in which a somatic mutation restores the open reading frame, restoring dystrophin expression in less than 1% of all muscle fibres[43]. This is a concern in assessment of contribution to regeneration measured by dystrophin positive myofibres following satellite cell transplantation. In order to visualize revertant fibres, and verify their prevalence in *mdx* host mice, immunohistochemistry was done on transverse cryosections of wildtype and *mdx* TA muscle. Dystrophin is shown to localize to the perimeter of myofibres (Figure 15). *Mdx* tissue virtually lacked dystrophin staining, except in rare revertant fibres. Isolated dystrophin positive myofibres were typically seen, although occasional clusters of two adjacent revertant fibres were also detected.

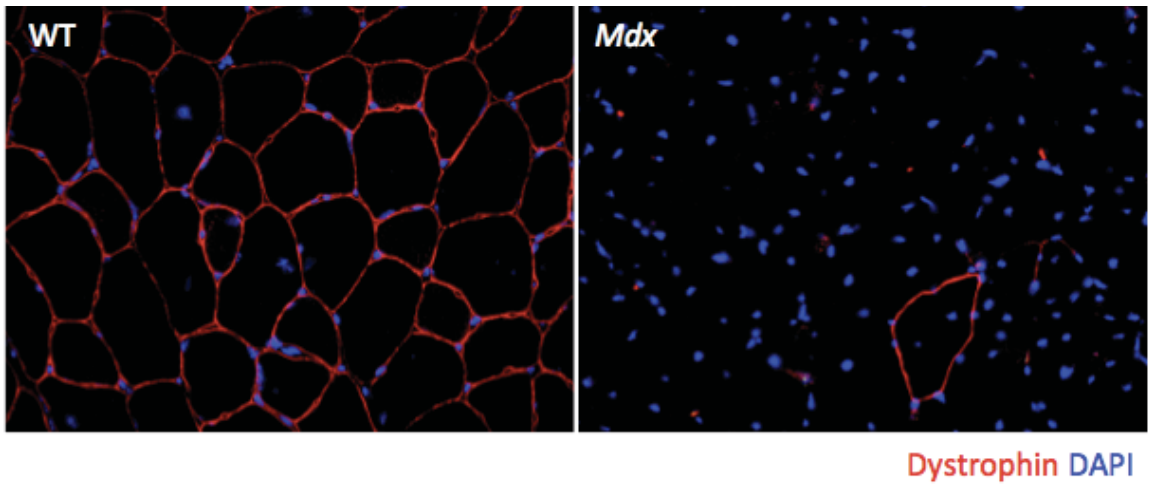

Figure 15: Dystrophin expression in wildtype and *mdx* mice. Transverse cryosections of *mdx* and wildtype TA muscle were immunolabeled with dystrophin (red). Images were merged over DAPI stained nuclei. The dystrophin positive myofibre in the *mdx* tissue is a revertant fibre.

Effects of Cardiotoxin Injection on Dystrophin Expression

One concern that arose during development of the engraftment assay was the possibility that induction into regeneration by cardiotoxin could be sufficient to increase the proportion of dystrophin positive myofibres compared to contralateral control tissue. Recently, Pigozzo *et al.* provided evidence that the increase in dystrophin positive fibres with age may be due, at least in part, to clonal expansion[37]. Furthermore, it was noted that even distant dystrophin positive myofibres could be clonal in origin due to migration of satellite cells[37]. Conversely, insignificant difference was reported in the percentage of dystrophin positive myofibres in TA and EDL muscle of *mdx* mice following cardiotoxin injury ($p > 0.05$, paired *t* test, n=20)[105]. However, this experiment involved injection of 20µl of 1µg/µl (equal to 1.428nM[106]) cardiotoxin at 9, 11, 13 and 15 weeks of age; whereas our methodology involved injection of 40µl of 10µM at 6 weeks of age. Due to these differences the effect of cardiotoxin alone was tested within our engraftment assay design. Cardiotoxin was not found to significantly increase the number of dystrophin positive myofibres relative to the untreated contralateral control TA muscle (Figure 16).

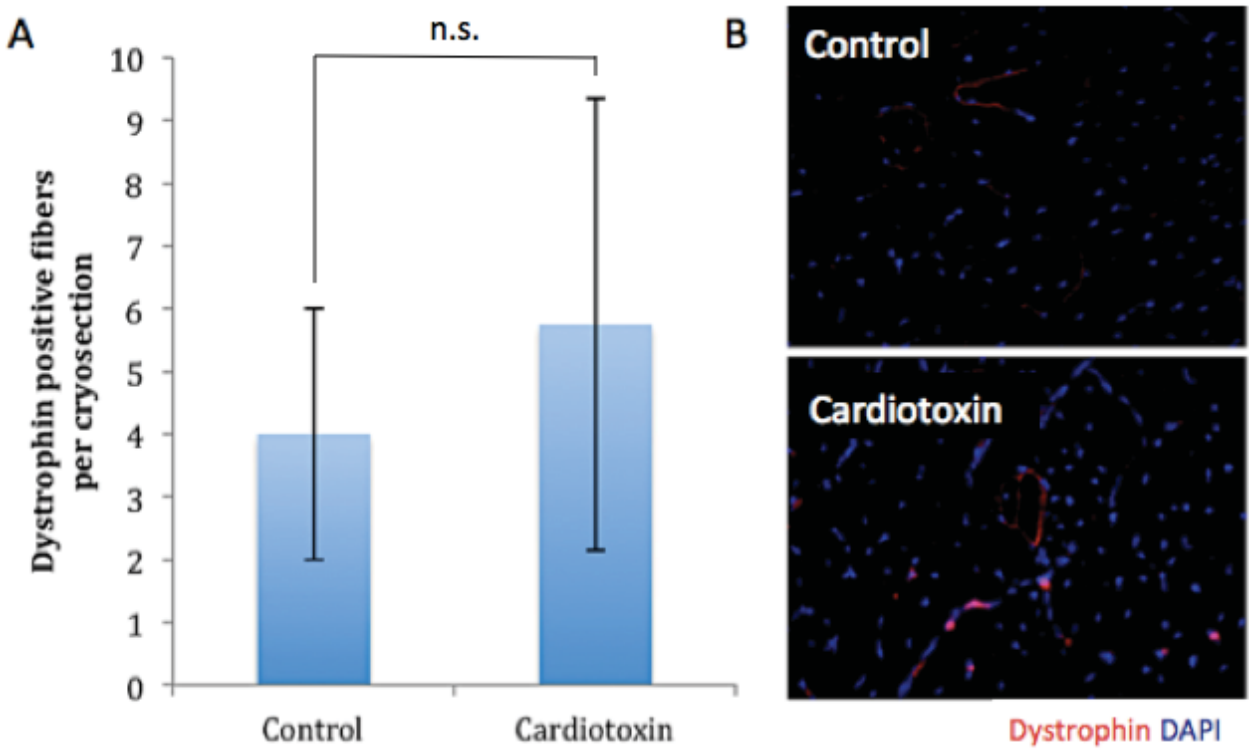

Figure 16: Cardiotoxin injury alone does not affect dystrophin restoration in muscle of *mdx* mice. A) The number of dystrophin positive "revertant" myofibres per cryosection was compared (n=4, p=0.4798). B) Immunolabeling for dystrophin (red), merged over DAPI stained nuclei, revealed dystrophin positive myofibres in the cardiotoxin injected and contralateral control TAs.

Untreated Myofibre Transplantation

Transplantation of single myofibres was performed in order to determine the engraftment efficiency of satellite cells with their native myofibre environment intact. Single myofibres are more economical to collect than satellite cells, since no flow cytometry is required. If transplantation of single myofibres resulted in greater restoration of dystrophin expression compared to transplantation of satellite cells, transfection of single myofibres with miR-31 could be done to determine the effect of miR-31 on engraftment.

Transplantation of single untransfected myofibres and their resident satellite cells resulted in an approximate 2-fold to 3-fold increase in the number of dystrophin positive myofibres in host tissue (Figure 17). Myofibres were obtained from Myf5^{nLacZ} mice in order to detect donor derived satellite cells, myoblasts, and myogenic precursors based on β-Galactosidase (β-Gal) activity following incubation with X-Gal solution[103]. No β-Gal

positive nuclei were detected, however; indicating that while transplantation lead to dystrophin restoration, no donor derived satellite or myogenic cells remained at the 3-week time point.

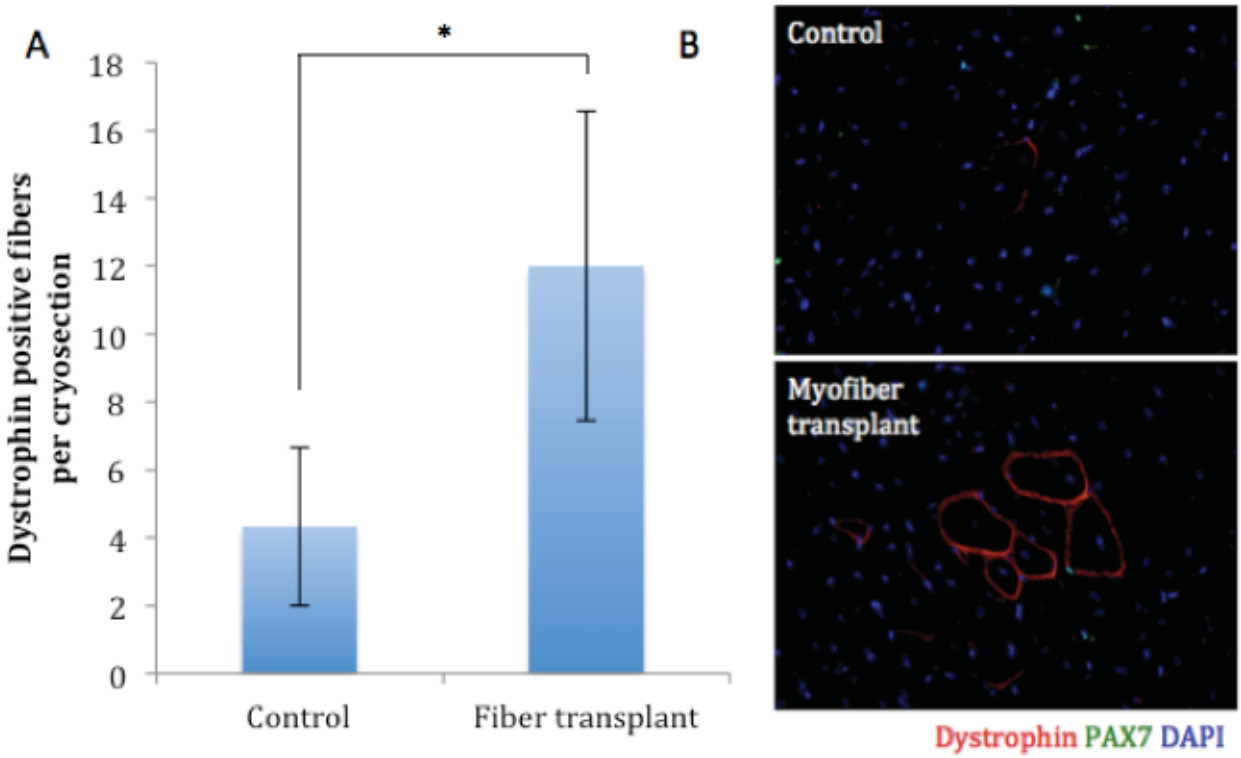

Figure 17: Transplantation of single untransfected myofibres isolated from *Myf5*$^{nLacz/+}$ mice into the tibialis anterior muscle of *mdx* mice immunosuppressed with FK506. A) The number of dystrophin positive myofibres per cryosection was compared (n=6, p=0.0014). B) Immunolabeling for dystrophin (red), and PAX7 (green), merged over DAPI-stained nuclei, revealed dystrophin positive myofibres and satellite cells.

Untreated Satellite Cell Transplantation

Approximately 15,000 freshly isolated satellite cells were transplanted in 5µl of satellite cell medium -P/S using a glass syringe. Four weeks after transplantation, TA muscles were pre-fixed and embedded in OCT. This protocol increased the clarity of dystrophin detection by immunofluorescence. Satellite cell transplantation gave a 2-fold increase in dystrophin positive myofibres (Figure 18), similar to the results of the single myofibre transplantation experiment (Figure 17).

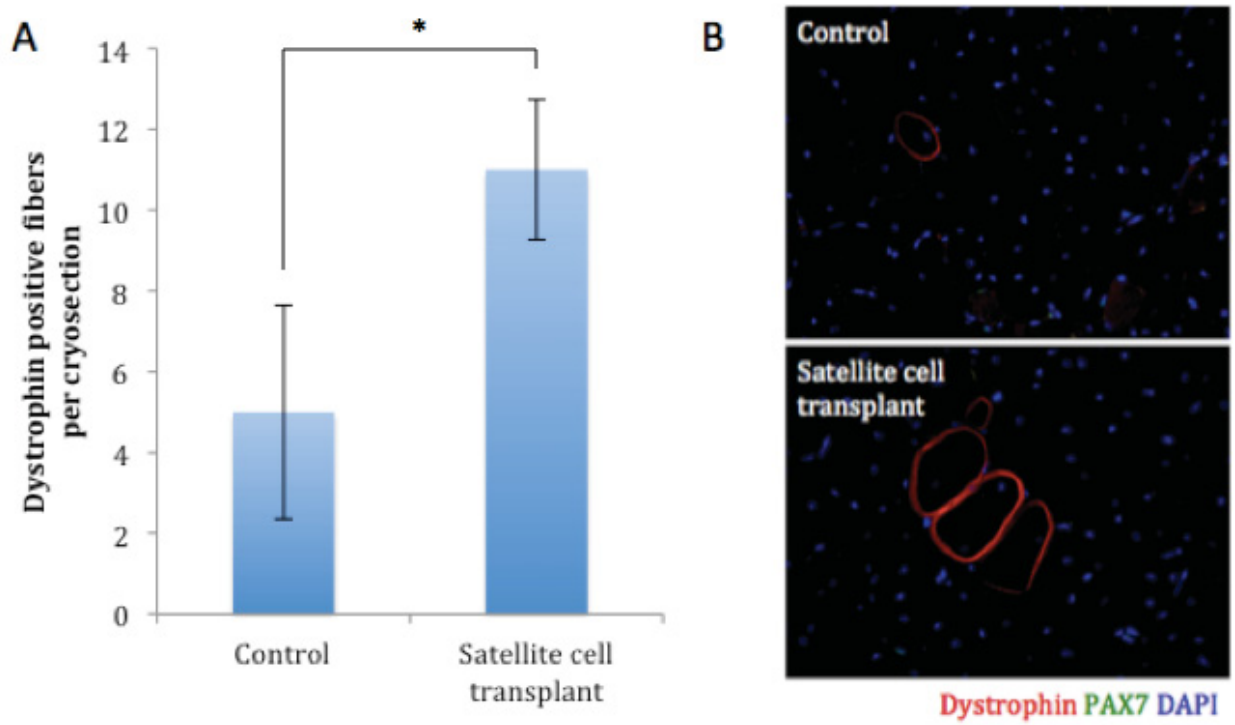

Figure 18: Transplantation of untreated satellite cells, isolated from muscle of *Pax3*$^{GFP/+}$ mice, into the tibialis anterior muscle of *mdx* mice immunosuppressed with FK506. A) The number of dystrophin positive myofibres per cryosection increased significantly with transplantation of satellite cells; p=0.0091, n=3 mice. B) Immunolabeling for Dystrophin (red), and PAX7 (green) merged over DAPI stained nuclei revealed dystrophin positive myofibres and satellite cells.

Transplantation of miR-31 and Control Satellite Cells into Irradiated Nude Dystrophic Hosts

Three to 7.5 week old *Foxn1*$^{nu/nu}$*; mdx* mice received 18Gy of irradiation directed towards their right hindlimb. Following irradiation, all mice were capable of bearing weight on the irradiated hindlimb. Then *Pax3*$^{GFP/+}$ tg(Actb-luc) satellite cells were isolated by flow cytometry, and transfected with miR-31 (mirVANA™) or negative control for 4 hours on ice. Fifteen thousand satellite cells per mouse were concentrated into 10ul of media, and transplanted into the right TA muscle with a glass syringe. At days 7, 14, and 21, *in vivo* bioluminescence imaging was used to monitor the engraftment. Efficient engraftment of satellite cells is often achieved with irradiated nude-*mdx* hosts[92]. Since this model incorporated irradiation with nude immunodeficiency, it was expected to facilitate engraftment.

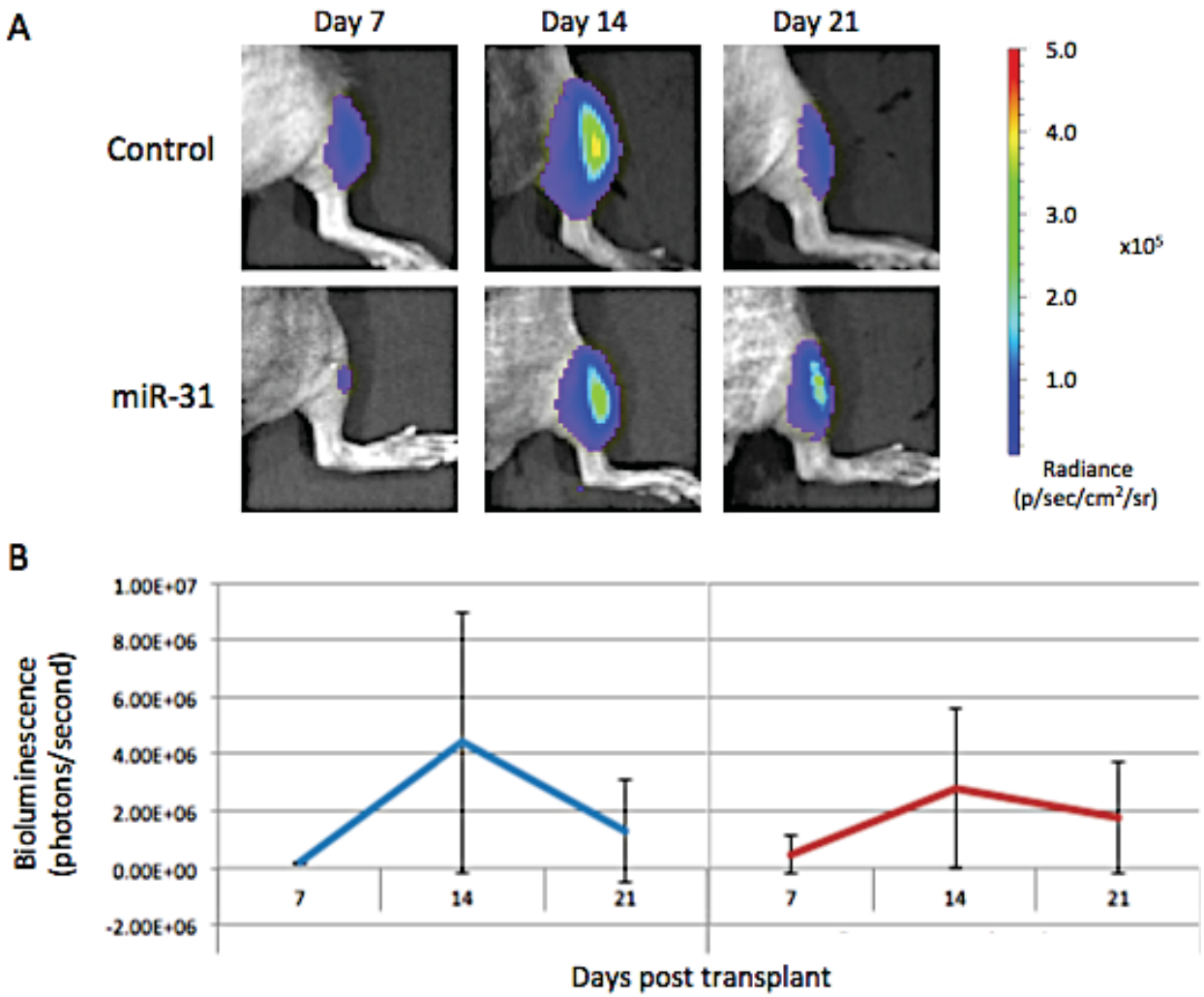

Figure 19: *In vivo* evidence of engraftment after control and miR-31 transfected satellite cells transplanted into the irradiated *tibialis anterior* muscle of immunocompromised *Foxn1*$^{nu/nu}$*; mdx* mice. A) Bioluminescence images from right hindlimbs that received transplantation of 15000 satellite cells isolated from the muscle of *Pax3*$^{GFP/+}$*; tg(actb-luc)* mice, at day 7, 14, and 21 post-transplant, as indicated. Legend bar to the right indicates the bioluminescence emitted by donor luciferase-expressing cells following administration of D-luciferin solution, measured in photons per second per cm^2 per steradian, correlating to the number of transplanted cells. B) Graphical representation of the changes in bioluminescence signal over time. Bioluminescence signal was maintained throughout the 3-week period of the engraftment assay. N=4 mice per transfection condition.

In order to determine whether the population of engrafted donor-derived *Pax3*$^{GFP/+}$ *tg(Actb-luc)* positive cells included satellite cells, immunofluorescence was performed. Detection of PAX7+/GFP+ cells would indicate self-renewing satellite cells of donor origin. TA muscles were collected at day 21 post transplant, pre-fixed and embedded in OCT.

Cryosections of 7μm thickness were taken and immunolabeled for PAX7 and GFP, as well as DAPI. Donor-derived satellite cells, marked by both GFP and PAX7, were rarely detected (at a rate of 5 or less per cryosection) (Figure 20). The total number of PAX7+ satellite cells detected in irradiated tissue was significantly decreased compared to the contralateral control tissue, as expected. It was hypothesized that transfection with miR-31 would increase the number of donor-derived satellite cells capable of self-renewal 21 after transplantation; however, this was not the case.

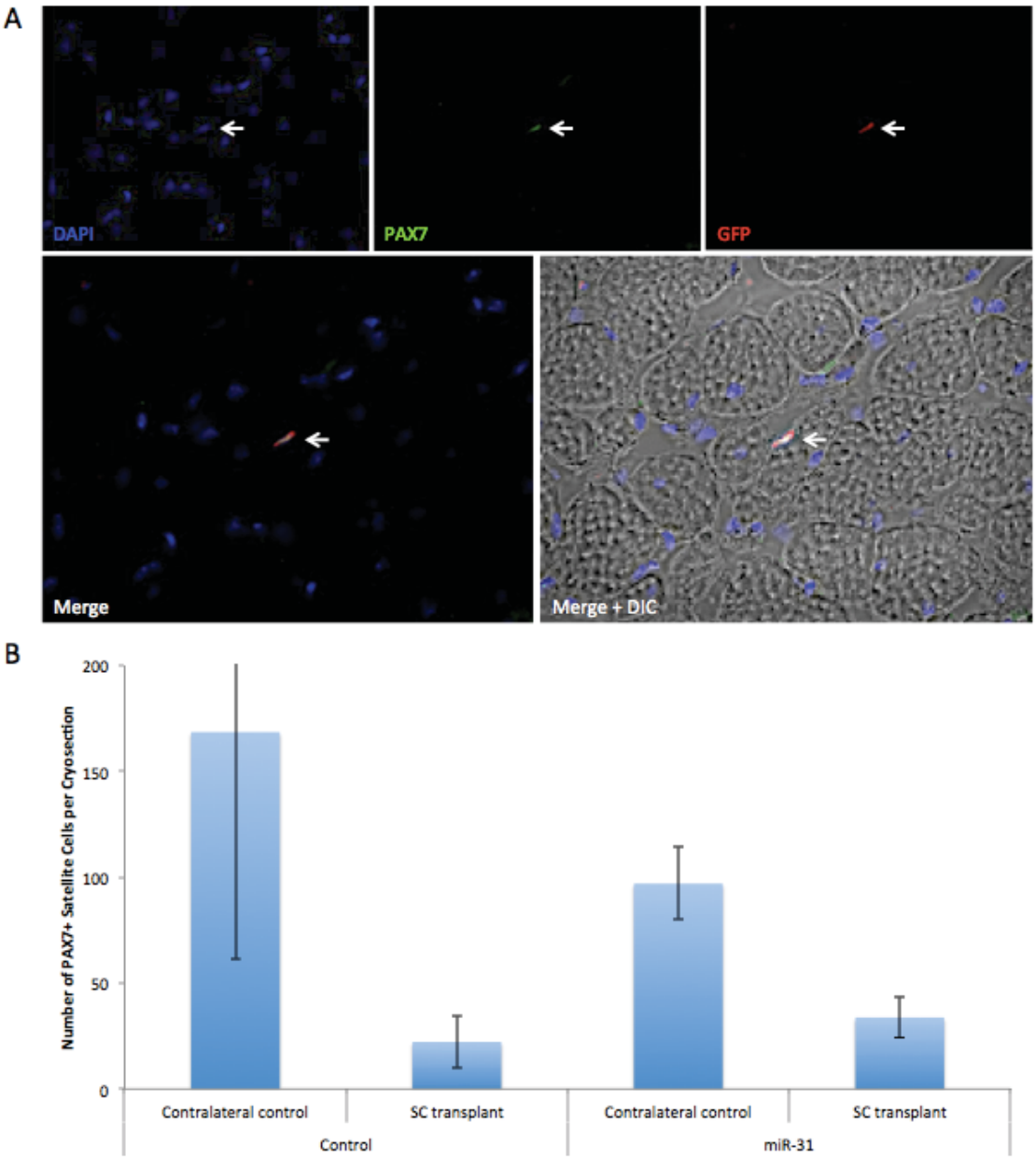

Figure 20: Detection of self-renewing satellite cells of donor origin after control and miR-31 transfected satellite cells, isolated from the muscle of *Pax3*$^{GFP/+}$*; tg(actb-luc)* mice, were transplanted into the *tibialis anterior* muscle of immunocompromised *Foxn1*$^{nu/nu}$*; mdx* mice. A) PAX7+/GFP+ cells were detected in small numbers in some of the TA cryosections whether they received control or miR-31 transfected satellite cells. A representative image is shown, obtained from muscle which received transplantation of control transfected satellite cells. The white arrow indicates a PAX7+/GFP+ satellite cell of donor origin. There was no significant difference between the numbers of PAX7+/GFP+ cells per transplanted cryosection, or the total number of satellite cells in the contralateral control tissue. B) The decrease in Pax7+GFP- satellite cells, of host origin, in irradiated muscle 21 days after engraftment, was highly significant based on two-way ANOVA; p=0.0024, n=4 mice per transfection condition.

Evidence of engraftment of satellite cells in nude-mdx mice can also be detected by restoration of dystrophin expression. This indicates contribution of donor-derived satellite cells, wildtype for Dystrophin expression, to regeneration of skeletal muscle tissue. Cryosections of 7μm thickness were taken and immunolabeled for PAX7 and Dystrophin, as well as DAPI. Large areas with restored dystrophin expression were detected in the samples that received both miR-31 and control transfected satellite cells (Figure 21). Revertant fibres were detected in contralateral control tissue, with no more than 2 adjacent dystrophin positive fibres in a cluster.

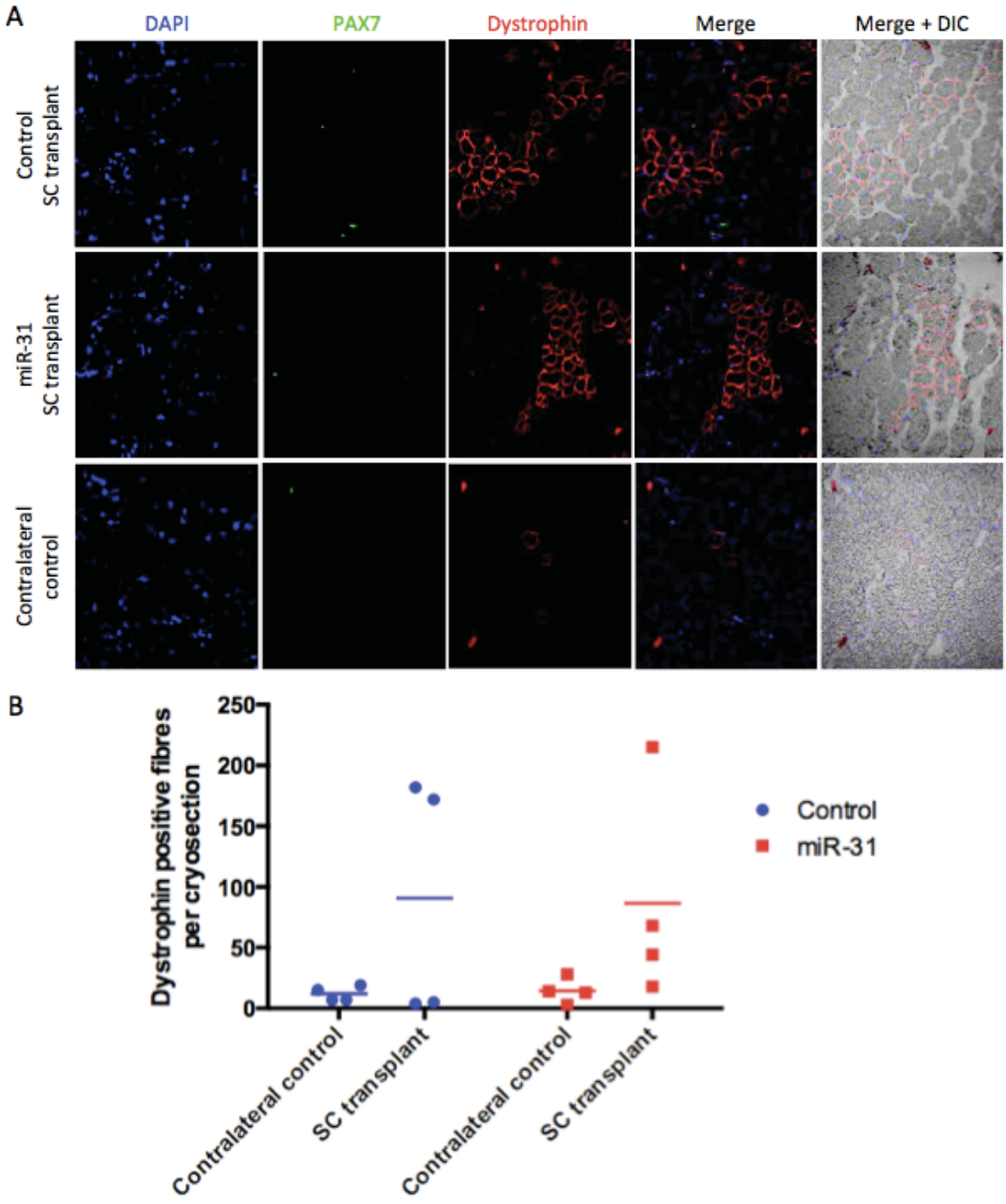

Figure 21: Restoration of dystrophin expression after control and miR-31 transfected satellite cells, isolated from the muscle of *Pax3*$^{GFP/+}$*; tg(actb-luc)* mice, were transplanted into the *tibialis anterior* muscle of immunocompromised *Foxn1*$^{nu/nu}$*; mdx* mice. A) Large areas of restored dystrophin expression were detected in TA cryosections, whether they received control or miR-31 transfected satellite cells. B) Graphical representation of results, with means indicated by horizontal lines. There was no significant difference between miR-31 and control transfection conditions in terms of dystrophin restoration. The increase in the number of dystrophin positive myofibres following satellite cell transplantation, regardless of transfection condition, is statistically significant based on two-way ANOVA; p=0.0438, n=4 mice per condition.

Development of a 4-Channel Immunolabeling protocol

It would be important to determine whether miR-31 transfected satellite cells are capable of contributing to regeneration, in addition to maintaining self-renewal. Nude-*mdx* mice could be used to detect the effects of miR-31 on dystrophin restoration in the TA muscle of immunodeficient hosts. It is possible to detect the presence of GFP+PAX7+ satellite cells in areas with dystrophin positive fibres using 3-channel immunofluorescence on serial cryosections. As an alternative, a 4-channel immunolabeling protocol was developed to allow staining of PAX7, dystrophin, GFP, and DAPI, all on the same cryosection (Figure 22). This method can be used in the future to determine whether PAX7+/GFP+ satellite cells are detected in areas with restored dystrophin expression.

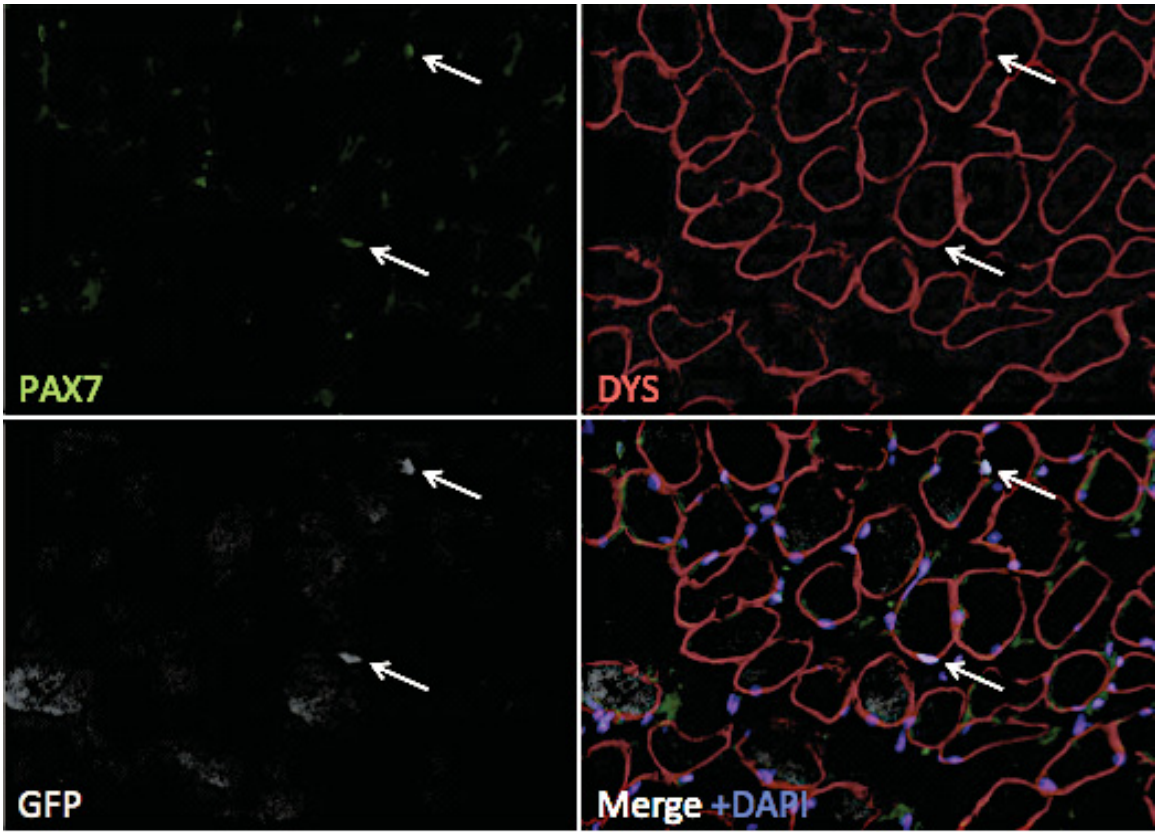

Figure 22: 4-channel immunolabeling protocol. Immunolabeling for PAX7 (green), GFP (pseudo-coloured gray), dystrophin (red), merged over DAPI (blue), on positive control diaphragm muscle from a *Pax3*$^{GFP/+}$ mouse. PAX7+/GFP+ satellite cells are indicated by white arrows.

Discussion

Effects of microRNA-31 on Self-Renewal of Satellite Cells

Lipid-mediated transfection of satellite cells with synthetic miR-31 results in a measurable increase in the level of miR-31 compared to control transfected satellite cells. By day 3 in culture, these increased levels of miR-31 result in an increase in the proportion of PAX7+/MYOD- cells. This satellite cell phenotype is associated with self-renewal, as well as homing to the satellite cell niche. The increase in PAX7+/MYOD- satellite cells was less significant in EDL myofibres than in cultured satellite cells. This could be due to limiting of the number of satellite cells by the myofibre, or less effective transfection through the basal lamina. However, the effect is still suggested among satellite cells along EDL myofibres, reinforcing the finding that miR-31 increase self-renewal of satellite cells.

It has been previously demonstrated that lipid-mediated transfection of satellite cells with miR-31 leads to a decrease in levels of MYF5, and a delay in progression through the myogenic program[18]. It has been reported that MYF5 becomes upregulated to compensate for knockout of MYOD[107]. Thus, it was postulated that MYOD expression could increase to compensate for the decrease in MYF5 induced by miR-31. However, this was not the case. Transfection with miR-31 lead to a decrease in PAX7-/MYOD+ activated satellite cells. Since there is no target site for miR-31 on the 3'UTR of *MyoD*, this finding suggests that miR-31 indirectly affects MYOD expression.

Effects of miR-31 on MYOD could be through the decrease in FXR1P, since *Fxr1* has been implicated in MYOD expression during zebrafish and Xenopus development[84, 85]. The genes targeted by MYOD are deregulated in FSHD myoblasts[108], supporting a role for FXR1 in altering levels of MYOD. Since *Fxr1* knockdown in myoblasts has been shown not to affect levels of *MyoD* transcript[87], the mechanism through which FXR1P affects MYOD is post-translational in nature. If exogenous expression of FXR1 following transfection of satellite cells with miR-31 reduces or reverses the increase in PAX7+/MYOD- cells at day 3 in culture, the effect of miR-31 on MYOD through FXR1 would be supported.

The *in vitro* culture conditions lack elements of the satellite cell niche. These elements include the pliable substrate of the myofibre, and signals from nearby blood

vessels and other cells. In the absence of signals from the satellite cell niche, levels of miR-31 are expected to decrease over time. Levels of miR-31 in miR-31 transfected satellite cells remain high, while levels of control transfected satellite cells decrease. Increased self-renewal of miR-31 transfected satellite cells in culture, under these conditions, supports a role for miR-31 in self-renewal of satellite cells *in vivo*. Alternatively, the effect of miR-31 on self-renewal of satellite cells could be assessed by knockdown of miR-31. Satellite cells could be transfected with mirVANA™ miRNA inhibitors *in vitro* to determine to what extent the proportion of self-renewing satellite cells is decreased. To determine the importance of miR-31 *in vivo*, antagomiR antisense miR-31 could be delivered systemically in mice[109], followed by assessment of defects in numbers of quiescent satellite cells and skeletal muscle tissue physiology.

Effects of microRNA-31 on FXR1 Expression in Satellite Cells

The *Fxr1* transcript was detected by 3'RACE in satellite cells at day 3, but not at 5 in culture. The primers amplified two isoforms, with alternative splicing of exon 16, but both contained the target site for miR-31 within the 3'UTR. Results of the luciferase assay verified that synthetic miR-31 is capable of binding to the seed region of the 3'UTR of Fxr1, inhibiting its translation. Preliminary experiments to transfect satellite cells with miR-31 resulted in a decrease in expression of FXR1P, particularly the muscle-specific isoform, at day 4 in culture. If these results are repeated and validated with siRNA experiments against the muscle specific isoform of Fxr1, they would support an effect of miR-31 transfection on FXR1P expression in satellite cells and their progeny.

FXR1P has been shown to be highly regulated by several microRNAs; however, this was done in Dt40 chicken B cell lymphoma cells, in which miR-31 is not expressed[110]. Satellite cells have been identified as a model in which this effect can be tested. Inhibition of miR-31 in satellite cells is expected to increase levels of FXR1P, and muscle specific isoforms in particular. This result would confirm that miR-31 is capable of supressing FXR1P levels, and that it does so in satellite cells. Additionally, the effect of Dicer knockdown could be compared to the effect of miR-31 inhibition in order to determine whether other miRNAs also target FXR1P in satellite cells. If this is the case, miRNAs with

predicted target sites on Fxr1 could be checked against the list of miRNAs differentially expressed in FSHD.

Expression of miR-31 is increased 1.76 fold in myoblasts of FSHD patients[89]. The presented research suggests that miR-31 decreases the levels of the muscle specific isoforms of FXR1P in satellite cells. Expression of these isoforms is reduced in FSHD patients[86]. It would follow that reducing the levels of miR31 in FSHD patients could alleviate the reduced expression of muscle specific FXR1P. However, little is known about the function of FXR1P, and its importance in FSHD.

Finally, recent evidence supports a role for the ~84 kDa isoform of FXR1P (Isoe) in inducing premature cell cycle arrest in FSHD myoblasts, which may explain the FSHD phenotype[87]. In the absence of FXR1P Isoe, p21 mRNA stability is increased, and its expression leads to premature cell cycle exit in myoblasts[87]. Davidovic *et al.* demonstrated an increase in the G0/G1 peak in siFxr1 treated C2C12s[87]. The presented western blot data suggests that lipid mediated transfection with miR-31 decreases ~84 kDa FXR1P. Cell cycle profiling did not demonstrate an increase in G0/G1 cells at day 3 of satellite cell culture; however, an increase in G0/G1 cells among miR-31 transfected cells would be predicted at day 5 in culture, indicating increased terminal differentiation.

Effects of microRNA-31 on Proliferation of Satellite Cells

Based on EdU incorporation at day 3 in culture, miR-31 does not appear to have an effect on the overall proliferation rate. The increase in self-renewing, non-activated satellite cells with miR-31 could be due to: delayed entry into the cell cycle upon plating; a return to quiescence; or slower cell cycle time, which would slow down the process of proliferation through asymmetric cell division. Both terminally differentiated myoblasts and quiescent satellite cells would be EdU negative. EdU labeling could be done in the 647nm channel to accommodate addition of immunolabeling to detect MYOD in the 594nm channel. This would allow detection of proliferation among PAX7+/MYOD-, PAX7+/MYOD+, PAX7-/MYOD+, and PAX7-/MYOD- cells. While PAX7+/MYOD- cells and PAX7-/MYOD- cells would include quiescent satellite cells and terminally differentiated myoblasts respectively, the intermediate cell phenotypes could be assessed for a shift in proliferation.

DNA staining with PI was used to perform cell cycle analysis by flow cytometry. There was no apparent difference in the proportion of G0/G1 or G2/M stage cells in miR-31 *versus* control transfected satellite cell progeny at day 3 in culture. A slight increase in the proportion of S phase cells was detected. This suggests increased entry into S phase, or prolonged duration of S phase[111]. However, the difference was not large enough to be considered definitive. Furthermore, the lack of a decrease in the G0/G1 peak suggests that miR-31 does not facilitate entry into S phase, while the lack of a decrease in the G2/M peak suggests that miR-31 does not inhibit S phase completion. When EdU incorporation was assessed by flow cytometry at day 3 in culture, no major difference was detected in the distribution of EdU labeling as a function of DNA content. This indicates that the cells that proliferated during the 4-hour window of EdU exposure did not encounter abnormal arrest at any of the stages of the cell cycle.

The results of the EdU incorporation and cell cycle profiling assays support rejection of the hypothesis that the denser clusters of cells in miR-31 transfected plates of satellite cells are caused by proliferation. Another potential cause of the denser clusters of cells is impaired cell migration. The doublets of cells seen in miR-31 transfected plates could be explained by reduced migration rate following cytokinesis. Cells could be tracked with live cell imaging video to determine their migration rate.

As myoblasts differentiate in culture, they undergo apoptosis. Slower terminal differentiation of *MyoD*$^{-/-}$ myoblasts appears to be protective against apoptosis[15]. Compared to wildtype myoblasts, *MyoD*$^{-/-}$ myoblasts exhibit increased expression of anti-apoptosis genes, as well as downregulation of genes contributing to apoptosis, resulting in a decrease in apoptosis measured by annexin-V staining[15]. Decreased levels of MYOD, due to transfection with miR-31, may have a similar affect on apoptosis, which could also explain the denser colonies of cells on miR-31 transfected plates at day 3 of satellite cell culture. Apoptosis could be tested by a terminal deoxynucleotidyl transferase dUTP nick end labeling assay, or annexin-V staining.

Myf5 is among thousands of predicted mRNA targets of miR-31[82]. Among candidates with mirSVR scores of predicted miR-31 targeting over -1.10, and with function keywords including proliferation, differentiation, cell cycle, apoptosis, and cell migration; Ttpa, Cops2, Foxc2, TCF4, Arid4a, Insc, Cntf, Tgfb2, and Pak1 lead to identification of

articles in PubMed when searched along with the term ("satellite cells" OR myoblasts). In order to ascertain which mRNAs are targeted by miR-31 in satellite cells, microRNA-bound mRNA capture could be performed. In this approach, cells are transfected with a biotinylated version of the microRNA, then a streptavidin pull-down is done to collect the microRNA along with the associated mRNAs[75]. Upon determination that apoptosis or cell migration of satellite cells is affected by miR-31, these candidate genes could be assessed as potential mediators.

Effects of microRNA-31 on Engraftment of Satellite Cells

Transfection of satellite cells with miR-31 helps retain self-renewal of satellite cells in culture. The ability of miR-31 transfected satellite cells to retain self-renewal upon transplantation is an important aspect of their potential use in therapy. In initial experiments, untreated satellite cells (Figure 19), or untreated single EDL myofibres with intact satellite cells (Figure 18), were transplanted into cardiotoxin injured TA muscle of *mdx* mice immunosuppressed with the drug FK-506. This protocol was implemented from an article in which transplantation of 15,000 satellite cells into mice immunosuppressed with FK-506, and induced into regeneration with cardiotoxin, resulted in detection of donor derived satellite cells[100]. At day 21 post-transplantation, control-transfected satellite cells resulted in detection of approximately 15 donor-derived PAX7+ satellite cells per mm^2[100]. The cross-sectional area of mouse TA muscle within the range of approximately 1.75-2.5 mm^2[112], so approximately 30 PAX7+GFP+ donor-derived satellite cells should have been detected in each cryosection of the TA that received transplantation of control-transfected satellite cells. Dystrophin expression was not reported in this paper[100].

Differences between this paper and the presented research were the re-suspended of satellite cells in sterile 0.9% NaCl for transplantation, rather than medium; tracking of donor derived cells by Pax7-zsGreen rather than $Pax3^{GFP/+}$; and the use of wildtype versus *mdx* hosts[100]. Since donor-derived satellite cells have been detected following transplantation in culture medium[103], attention is turned to the method of tracking satellite cells, and the host environment. While PAX7 is expressed in all satellite cells of TA muscle, PAX3 is only expressed in satellite cells of other muscle groups in the adult. It is

possible that activation of Pax3$^{GFP/+}$ satellite cells results in loss of GFP expression, while activation would not impact zsGreen expression in Pax7-zsGreen satellite cells. Finally, the reference experiment was done in wildtype hosts[100], while the presented work involved transplantation into *mdx* mice. The difference in results supports the hypothesis that a dystrophic host environment is a barrier to engraftment.

A point of difference between satellite cell engraftment assays in the literature is the number of transplanted cells. To demonstrate the breadth of variation between protocols, *in vivo* bioluminescence imaging has been used to detect engraftment of a mix of 1,000,000 satellite cells and myoblasts[15], and of a single satellite stem cell[65]. Although diverging methods make it difficult to compare the two experiments, transplantation of 1,000,000 heterogeneous myogenic cells did not result in much greater engraftment. If transplanted satellite cells are capable of long-term self-renewal, the initial number of transplanted satellite cells is a lesser concern. Mechanisms to maintain self-renewal, including transfection with miR-31, are therefore an important contribution to engraftment assays.

In the subsequent *in vivo* imaging experiment, transplantation of miR-31 and control transfected Pax3$^{GFP/+}$ β-actin^{Luc} satellite cells was done to allow detection of donor-derived cells *in vivo* by Luciferase bioluminescence, detection of donor derived self-renewing satellite cells by immunohistochemistry for PAX7 and GFP, and detection of contribution to regeneration by immunohistochemistry for Dystrophin. Nude-*mdx* hosts were used in accordance with the literature[30, 92, 102]. Transient transfection of donor satellite cells with miR-31 did not have statistically significant effect on expansion of donor-derived cells analyzed by *in vivo* bioluminescence imaging, restoration of dystrophin expression or self-renewal of donor derived satellite cells. As proof of concept, future experiments that address whether or not transient miR-31 transfections increase the expansion and/or self-renewal of engrafted satellite cells might be done in nude mice without the *Dmd* mutation (*mdx*) since the dystrophic environment is detrimental to the long term engraftment potential of satellite cells.

The effects of miR-31 on engraftment of satellite cells should be compared to other approaches to increase self-renewal in a standardized engraftment assay. Improved engraftment of satellite cells have been achieved following culture in 4% oxygen[69], as well as culture on 12 kPa hydrogel coated plates[65], have been shown to improve

engraftment efficiency. Satellite cells could be cultured for 3 days with 4% oxygen, on a 12 kPa hydrogel coated plate, or with miR-31 transfection medium. The approaches could be combined to determine whether their effects are additive or synergistic. Hypoxia increases self-renewal through activation of the Notch signalling pathway, which represses miR-1 and miR-206 to increase PAX7 expression[69]. The pathways activated by culture on 12 kPa hydrogel coated plates remain unknown[64]. The presented research has shown that miR-31 increases self-renewal *in vitro* through targeting of *Myf5*, and possibly indirect downregulation of MYOD. The effects of hypoxia and transfection with miR-31 are expected to at least be additive. All combinations of approaches could be tested by detection of the proportion of self-renewing PAX7+/MYOD- satellite cells at day 3 in culture. The number of PAX7+/MYOD- cells could be divided by the number of plated cells in order to determine efficiency of *ex-vivo* expansion. If miR-31 promotes *ex-vivo* expansion of satellite cells, rather than just maintaining their proportion for longer in culture, miR-31 could address the difficulty of expanding satellite cells from donors for cell therapy.

The advantage of miR-31 transfection over the other approaches mentioned is that prolonged culture is not required, reducing the time satellite cells have to differentiate *ex vivo* to 4 hours on ice. It would be essential to compare the effects of miR-31 transfection to transplantation of satellite cells immediately following isolation by flow cytometry, rather than just to control-transfected satellite cells. Freshly isolated satellite cells were used in the engraftment experiments used to develop the engraftment assay, but were not included as a control group in the pilot engraftment experiment or *in vivo* bioluminescence experiments using irradiated *mdx* and nude-*mdx*/+ mice. Demonstration of enhanced engraftment of miR-31-transfected satellite cells relative to freshly isolated satellite cells would bolster their therapeutic potential.

Whether satellite cells are obtained from patients for *ex vivo* correction of dystrophin expression, or obtained from match donors, a limiting factor in satellite cell transplantation assays is the number of satellite cells that can be obtained by muscle biopsy. On the other hand, myogenic cells could be derived from induced pluripotent stem cells, and genetically corrected to restore dystrophin expression, for autologous cell therapy to treat DMD. PAX7 expressing “satellite-like” cells have previously been generated from pluripotent embryonic cells marked by GFP expression[26]. Following

transplantation into irradiated *mdx* mice induced into regeneration with cardiotoxin, GFP positive tissue and GFP+/PAX7+ cells were detected in host muscle[26]. The presented research indicates that miR-31 expression may improve engraftment and long-term self-renewal of myogenic stem cells generated from pluripotent cells. It would be interesting to determine whether these cells express miR-31 upon engraftment into the satellite cell niche, and whether transfection with miR-31 improves their engraftment efficiency.

Conclusion

Lipid-mediated transfection of satellite cells with synthetic microRNA-31 leads to vastly increased levels of miR-31 by qPCR. This increase in microRNA-31 is met with an increase in PAX7+/MYOD- self-renewing satellite cells at day 3 in culture. Transfection with synthetic miR-31 results in decreased levels of FXR1P exogenously expressed in HEK 293 cells, and appears to do the same in satellite cells at day 4 in culture. Further experimentation is required to determine whether the decrease in MYOD expression is secondary to the decrease in FXR1P, and whether decreased FXR1 alters cell cycle of satellite cells. Transplanted *Pax3*$^{GFP/+}$ satellite cells transfected with synthetic microRNA-31, as well as control microRNA mimic, have been shown to expand *in vivo* following transplantation into the TA muscle of irradiated nude-*mdx* mice. Both transfection conditions resulted in detection of rare PAX7+/GFP+ satellite cells of donor origin at the perimeter of myofibres at day 21 after engraftment. Both transfection conditions resulted in detection of large areas of restored dystrophin expression at day 21 after engraftment. While engraftment of transplanted satellite cells was successful, no significant increase in self-renewal was attributed to transfection with synthetic miR-31. Transplantation of miR-31 and control transfected satellite cells should be repeated in irradiated nude non-dystrophic host mice to allow higher levels of engraftment, and thereby increased resolution to detect the effects of miR-31 on self-renewal *in vivo*.

References

1. Hill, J.A. and E.N. Olson, *Chapter 1 - An Introduction to Muscle*, in *Muscle*, J.A. Hill and E.N. Olson, Editors. 2012, Academic Press: Boston/Waltham. p. 3-9.
2. Scime, A., A.Z. Caron, and G. Grenier, *Advances in myogenic cell transplantation and skeletal muscle tissue engineering.* Front Biosci (Landmark Ed), 2009. **14**: p. 3012-23.
3. Cohen, B.J., *Memmler's The Human Body in Health and Disease*. 12 edition ed. 2013: Lippincott Williams & Wilkins.
4. Relaix, F. and P. Zammit, *Satellite cells are essential for skeletal muscle regeneration: the cell on the edge returns centre stage.* Development, 2012. **139**(16): p. 2845-2856.
5. Buckingham, M. and A. Mayeuf, *Chapter 52 - Skeletal Muscle Development*, in *Muscle*, J.A. Hill and E.N. Olson, Editors. 2012, Academic Press: Boston/Waltham. p. 749-762.
6. Collins, C.A., et al., *Stem cell function, self-renewal, and behavioral heterogeneity of cells from the adult muscle satellite cell niche.* Cell, 2005. **122**(2): p. 289-301.
7. Guttridge, D.C., *Chapter 65 - Skeletal Muscle Regeneration*, in *Muscle*, J.A. Hill and E.N. Olson, Editors. 2012, Academic Press: Boston/Waltham. p. 921-933.
8. Hawke, T.J. and D.J. Garry, *Myogenic satellite cells: physiology to molecular biology.* J Appl Physiol (1985), 2001. **91**(2): p. 534-51.
9. McKinnell, I., et al., *Pax7 activates myogenic genes by recruitment of a histone methyltransferase complex.* Nature Cell Biology, 2008. **10**(1): p. 77-84.
10. Lepper, C., T.A. Patridge, and C.-M. Fan, *An absolute requirement for Pax7-positive satellite cells in acute injury-induced skeletal muscle regeneration.* Development, 2011. **138**(17): p. 3639.
11. Peault, B., et al., *Stem and progenitor cells in skeletal muscle development, maintenance, and therapy.* Mol Ther, 2007. **15**(5): p. 867-77.
12. Kuang, S., et al., *Distinct roles for Pax7 and Pax3 in adult regenerative myogenesis.* J Cell Biol, 2006. **172**(1): p. 103-13.
13. Sambasivan, R., et al., *Pax7-expressing satellite cells are indispensable for adult skeletal muscle regeneration.* Development, 2011. **138**(17): p. 10.
14. Giordani, L. and P.L. Puri, *Epigenetic control of skeletal muscle regeneration: Integrating genetic determinants and environmental changes.* Febs j, 2013. **280**(17): p. 4014-25.
15. Asakura, A., et al., *Increased survival of muscle stem cells lacking the MyoD gene after transplantation into regenerating skeletal muscle.* Proc Natl Acad Sci U S A, 2007. **104**(42): p. 16552-7.
16. Sabourin, L.A. and M.A. Rudnicki, *The molecular regulation of myogenesis.* Clin Genet, 2000. **57**(1): p. 16-25.
17. Soleimani, V.D., et al., *Snail regulates MyoD binding-site occupancy to direct enhancer switching and differentiation-specific transcription in myogenesis.* Mol Cell, 2012. **47**(3): p. 457-68.
18. Crist, C.G., D. Montarras, and M. Buckingham, *Muscle satellite cells are primed for myogenesis but maintain quiescence with sequestration of Myf5 mRNA targeted by microRNA-31 in mRNP granules.* Cell Stem Cell, 2012. **11**(1): p. 118-26.
19. Gayraud-Morel, B., et al., *A role for the myogenic determination gene Myf5 in adult regenerative myogenesis.* Dev Biol, 2007. **312**(1): p. 13-28.

20. Gharaibeh, B., et al., *Chapter 62 - Musculoskeletal Tissue Injury and Repair: Role of Stem Cells, Their Differentiation, and Paracrine Effects*, in *Muscle*, J.A. Hill and E.N. Olson, Editors. 2012, Academic Press: Boston/Waltham. p. 881-897.
21. Turk, R., et al., *Muscle regeneration in dystrophin-deficient mdx mice studied by gene expression profiling.* BMC Genomics, 2005. **6**: p. 98.
22. Zammit, P.S., et al., *Muscle satellite cells adopt divergent fates: a mechanism for self-renewal?* J Cell Biol, 2004. **166**(3): p. 347-57.
23. Wen, Y., et al., *Constitutive Notch activation upregulates Pax7 and promotes the self-renewal of skeletal muscle satellite cells.* Mol Cell Biol, 2012. **32**(12): p. 2300-11.
24. He, W.A., et al., *NF-kappaB-mediated Pax7 dysregulation in the muscle microenvironment promotes cancer cachexia.* J Clin Invest, 2013. **123**(11): p. 4821-35.
25. Cerletti, M., et al., *Highly efficient, functional engraftment of skeletal muscle stem cells in dystrophic muscles.* Cell, 2008. **134**(1): p. 37-47.
26. Chang, H., et al., *Generation of transplantable, functional satellite-like cells from mouse embryonic stem cells.* FASEB J, 2009. **23**(6): p. 1907-19.
27. Kim, J.A.R., Roland R.; Edgerton, V. Reggie, *Chapter 55 - Neuromechanical Interactions that Control Muscle Function and Adaptation*, in *Muscle*, J.A. Hill and E.N. Olson, Editors. 2012, Academic Press: Boston/Waltham. p. 789-800.
28. Cheek, D.B., G.K. Powell, and R.E. Scott, *GROWTH OF MUSCLE MASS AND SKELETAL COLLAGEN IN THE RAT. I. NORMAL GROWTH.* Bull Johns Hopkins Hosp, 1965. **116**: p. 378-87.
29. Schofield, R., *The stem cell system.* Biomed Pharmacother, 1983. **37**(8): p. 375-80.
30. Boldrin, L., et al., *Mature adult dystrophic mouse muscle environment does not impede efficient engrafted satellite cell regeneration and self-renewal.* Stem Cells, 2009. **27**(10): p. 2478-87.
31. Conboy, I.M., et al., *Rejuvenation of aged progenitor cells by exposure to a young systemic environment.* Nature, 2005. **433**(7027): p. 760-4.
32. Joe, A.W., et al., *Muscle injury activates resident fibro/adipogenic progenitors that facilitate myogenesis.* Nat Cell Biol, 2010. **12**(2): p. 153-63.
33. Murphy, M., et al., *Satellite cells, connective tissue fibroblasts and their interactions are crucial for muscle regeneration.* Development, 2011. **138**(17): p. 3625.
34. *DMD dystrophin [Homo sapiens (human)]* 2014-05-12 2014-05-14]; Gene ID: 1756]. Available from: http://www.ncbi.nlm.nih.gov/gene/1756.
35. *Duchenne muscular dystrophy (DMD) Teacher Resource*, D.F. Australia, Editor. 2013: http://www.duchennefoundation.org.au.
36. Fairclough, R.J., M.J. Wood, and K.E. Davies, *Therapy for Duchenne muscular dystrophy: renewed optimism from genetic approaches.* Nat Rev Genet, 2013. **14**(6): p. 373-8.
37. Pigozzo, S.R., et al., *Revertant fibers in the mdx murine model of Duchenne muscular dystrophy: an age- and muscle-related reappraisal.* PLoS One, 2013. **8**(8): p. e72147.
38. Cacchiarelli, D., et al., *MicroRNAs involved in molecular circuitries relevant for the Duchenne muscular dystrophy pathogenesis are controlled by the dystrophin/nNOS pathway.* Cell Metab, 2010. **12**(4): p. 341-51.
39. Meregalli, M., et al., *Perspectives of stem cell therapy in Duchenne muscular dystrophy.* FEBS J, 2013. **280**(17): p. 4251-62.

40. Benedetti, S., H. Hoshiya, and F.S. Tedesco, *Repair or replace? Exploiting novel gene and cell therapy strategies for muscular dystrophies.* FEBS J, 2013. **280**(17): p. 4263-80.
41. McClorey, G., et al., *Antisense oligonucleotide-induced exon skipping restores dystrophin expression in vitro in a canine model of DMD.* Gene Ther, 2006. **13**(19): p. 1373-81.
42. Sacco, A., et al., *Short telomeres and stem cell exhaustion model Duchenne muscular dystrophy in mdx/mTR mice.* Cell, 2010. **143**(7): p. 1059-71.
43. Arechavala-Gomeza, V., et al., *Revertant fibres and dystrophin traces in Duchenne muscular dystrophy: implication for clinical trials.* Neuromuscul Disord, 2010. **20**(5): p. 295-301.
44. Partridge, T.A., *Impending therapies for Duchenne muscular dystrophy.* Curr Opin Neurol, 2011. **24**(5): p. 415-22.
45. Lavasani, M., et al., *Nerve growth factor improves the muscle regeneration capacity of muscle stem cells in dystrophic muscle.* Hum Gene Ther, 2006. **17**(2): p. 180-92.
46. Mitrpant, C., S. Fletcher, and S.D. Wilton, *Personalised genetic intervention for Duchenne muscular dystrophy: antisense oligomers and exon skipping.* Curr Mol Pharmacol, 2009. **2**(1): p. 110-21.
47. Aoki, Y., T. Yokota, and M.J. Wood, *Development of multiexon skipping antisense oligonucleotide therapy for Duchenne muscular dystrophy.* Biomed Res Int, 2013. **2013**: p. 402369.
48. Scime, A. and M.A. Rudnicki, *Molecular-targeted therapy for Duchenne muscular dystrophy: progress and potential.* Mol Diagn Ther, 2008. **12**(2): p. 99-108.
49. Hoffman, E.P., et al., *Restoring dystrophin expression in duchenne muscular dystrophy muscle progress in exon skipping and stop codon read through.* Am J Pathol, 2011. **179**(1): p. 12-22.
50. Tedesco, F.S., et al., *Stem cell-mediated transfer of a human artificial chromosome ameliorates muscular dystrophy.* Sci Transl Med, 2011. **3**(96): p. 96ra78.
51. Gussoni, E., et al., *Normal dystrophin transcripts detected in Duchenne muscular dystrophy patients after myoblast transplantation.* Nature, 1992. **356**(6368): p. 435-8.
52. Smythe, G.M., S.I. Hodgetts, and M.D. Grounds, *Immunobiology and the future of myoblast transfer therapy.* Mol Ther, 2000. **1**(4): p. 304-13.
53. Huard, J., et al., *Myoblast transplantation produced dystrophin-positive muscle fibres in a 16-year-old patient with Duchenne muscular dystrophy.* Clin Sci (Lond), 1991. **81**(2): p. 287-8.
54. Tremblay, J.P., et al., *Results of a triple blind clinical study of myoblast transplantations without immunosuppressive treatment in young boys with Duchenne muscular dystrophy.* Cell Transplant, 1993. **2**(2): p. 99-112.
55. Karpati, G., et al., *Myoblast transfer in Duchenne muscular dystrophy.* Ann Neurol, 1993. **34**(1): p. 8-17.
56. Vilquin, J.T., et al., *Cyclophosphamide immunosuppression does not permit successful myoblast allotransplantation in mouse.* Neuromuscul Disord, 1995. **5**(6): p. 511-7.
57. Mendell, J.R., et al., *Myoblast transfer in the treatment of Duchenne's muscular dystrophy.* N Engl J Med, 1995. **333**(13): p. 832-8.

58. Hodgetts, S.I. and M.D. Grounds, *Complement and myoblast transfer therapy: donor myoblast survival is enhanced following depletion of host complement C3 using cobra venom factor, but not in the absence of C5.* Immunol Cell Biol, 2001. **79**(3): p. 231-9.
59. Sacco, A., et al., *Self-renewal and expansion of single transplanted muscle stem cells.* Nature, 2008. **456**(7221): p. 502-6.
60. Darabi, R., et al., *Human ES- and iPS-derived myogenic progenitors restore DYSTROPHIN and improve contractility upon transplantation in dystrophic mice.* Cell Stem Cell, 2012. **10**(5): p. 610-9.
61. Morgan, J.E., et al., *Myogenic cell proliferation and generation of a reversible tumorigenic phenotype are triggered by preirradiation of the recipient site.* J Cell Biol, 2002. **157**(4): p. 693-702.
62. Sakai, H., et al., *Fetal skeletal muscle progenitors have regenerative capacity after intramuscular engraftment in dystrophin deficient mice.* PLoS One, 2013. **8**(5): p. e63016.
63. Tedesco, F.S., et al., *Transplantation of genetically corrected human iPSC-derived progenitors in mice with limb-girdle muscular dystrophy.* Sci Transl Med, 2012. **4**(140): p. 140ra89.
64. Gilbert, P.M., et al., *A single cell bioengineering approach to elucidate mechanisms of adult stem cell self-renewal.* Integr Biol (Camb), 2012. **4**(4): p. 360-7.
65. Gilbert, P.M., et al., *Substrate elasticity regulates skeletal muscle stem cell self-renewal in culture.* Science, 2010. **329**(5995): p. 1078-81.
66. Parker, M.H., et al., *Activation of Notch signaling during ex vivo expansion maintains donor muscle cell engraftment.* Stem Cells, 2012. **30**(10): p. 2212-20.
67. Ogura, Y., et al., *Proinflammatory cytokine tumor necrosis factor (TNF)-like weak inducer of apoptosis (TWEAK) suppresses satellite cell self-renewal through inversely modulating Notch and NF-kappaB signaling pathways.* J Biol Chem, 2013. **288**(49): p. 35159-69.
68. Briggs, D. and J.E. Morgan, *Recent progress in satellite cell/myoblast engraftment -- relevance for therapy.* FEBS J, 2013. **280**(17): p. 4281-93.
69. Liu, W., et al., *Hypoxia promotes satellite cell self-renewal and enhances the efficiency of myoblast transplantation.* Development, 2012. **139**(16): p. 2857-65.
70. Li, G.W. and X.S. Xie, *Central dogma at the single-molecule level in living cells.* Nature, 2011. **475**(7356): p. 308-15.
71. Adeli, K., *Translational control mechanisms in metabolic regulation: critical role of RNA binding proteins, microRNAs, and cytoplasmic RNA granules.* Am J Physiol Endocrinol Metab, 2011. **301**(6): p. E1051-64.
72. Liu, N., et al., *microRNA-206 promotes skeletal muscle regeneration and delays progression of Duchenne muscular dystrophy in mice.* J Clin Invest, 2012. **122**(6): p. 2054-65.
73. Winter, J., et al., *Many roads to maturity: microRNA biogenesis pathways and their regulation.* Nat Cell Biol, 2009. **11**(3): p. 228-34.
74. Chan, Y.T., et al., *Concordant and discordant regulation of target genes by miR-31 and its isoforms.* PLoS One, 2013. **8**(3): p. e58169.
75. Lal, A., et al., *Capture of microRNA-bound mRNAs identifies the tumor suppressor miR-34a as a regulator of growth factor signaling.* PLoS Genet, 2011. **7**(11): p. e1002363.

76. Crist, C.G. and M. Buckingham, *Megarole for microRNA in muscle disease.* Cell Metab, 2010. **12**(5): p. 425-6.
77. Lund, T.C., R.W. Grange, and D.A. Lowe, *Telomere shortening in diaphragm and tibialis anterior muscles of aged mdx mice.* Muscle Nerve, 2007. **36**(3): p. 387-90.
78. Rao, P.K., et al., *Myogenic factors that regulate expression of muscle-specific microRNAs.* Proc Natl Acad Sci U S A, 2006. **103**(23): p. 8721-6.
79. Greco, S., et al., *Common micro-RNA signature in skeletal muscle damage and regeneration induced by Duchenne muscular dystrophy and acute ischemia.* Faseb j, 2009. **23**(10): p. 3335-46.
80. Roberts, T.C., et al., *Expression analysis in multiple muscle groups and serum reveals complexity in the microRNA transcriptome of the mdx mouse with implications for therapy.* Mol Ther Nucleic Acids, 2012. **1**: p. e39.
81. Cacchiarelli, D., et al., *miR-31 modulates dystrophin expression: new implications for Duchenne muscular dystrophy therapy.* EMBO Rep, 2011. **12**(2): p. 136-41.
82. *microRNA.org - Targets and Expression*.
83. Darnell, J.C., et al., *Discrimination of common and unique RNA-binding activities among Fragile X mental retardation protein paralogs.* Hum Mol Genet, 2009. **18**(17): p. 3164-77.
84. van't Padje, S., et al., *Reduction in fragile X related 1 protein causes cardiomyopathy and muscular dystrophy in zebrafish.* Journal of experimental biology, 2009. **212**(16): p. 2564.
85. Huot, M.-E., et al., *The RNA-binding Protein Fragile X-related 1 Regulates Somite Formation in Xenopus laevis.* Molecular biology of the cell, 2005. **16**.
86. Davidovic, L., et al., *Alteration of expression of muscle specific isoforms of the fragile X related protein 1 (FXR1P) in facioscapulohumeral muscular dystrophy patients.* Journal of Medical Genetics, 2008. **45**(10): p. 7.
87. Davidovic, L., et al., *A novel role for the RNA-binding protein FXR1P in myoblasts cell-cycle progression by modulating p21/Cdkn1a/Cip1/Waf1 mRNA stability.* PLoS Genet, 2013. **9**(3): p. e1003367.
88. Harafuji, N., et al., *miR-411 is up-regulated in FSHD myoblasts and suppresses myogenic factors.* Orphanet J Rare Dis, 2013. **8**: p. 55.
89. Dmitriev, P., et al., *Defective regulation of microRNA target genes in myoblasts from facioscapulohumeral dystrophy patients.* J Biol Chem, 2013. **288**(49): p. 34989-5002.
90. Collins, C.A. and P.S. Zammit, *Isolation and grafting of single muscle fibres.* Methods Mol Biol, 2009. **482**: p. 319-30.
91. Relaix, F., et al., *A Pax3/Pax7-dependent population of skeletal muscle progenitor cells.* Nature, 2005. **435**(7044): p. 948-53.
92. Montarras, D., et al., *Direct isolation of satellite cells for skeletal muscle regeneration.* Science, 2005. **309**(5743): p. 2064-7.
93. Montarras, D., A. L'Honore, and M. Buckingham, *Lying low but ready for action: the quiescent muscle satellite cell.* Febs j, 2013. **280**(17): p. 4036-50.
94. Gaster, M., H. Beck-Nielsen, and H.D. Schroder, *Proliferation conditions for human satellite cells. The fractional content of satellite cells.* Apmis, 2001. **109**(11): p. 726-34.
95. Gabillard, J.C., N. Sabin, and G. Paboeuf, *In vitro characterization of proliferation and differentiation of trout satellite cells.* Cell Tissue Res, 2010. **342**(3): p. 471-7.

96. *Lipofectamine™ 2000 Transfection Reagent*. Life Technologies.
97. *Gene: Fxr1 (ENSMUSG00000027680)*. 2014, US West: Ensembl.
98. Lin, P., et al., *Polybrene inhibits human mesenchymal stem cell proliferation during lentiviral transduction.* PLoS One, 2011. **6**(8): p. e23891.
99. *Propidium iodide staining of cells to assess DNA cell cycle*, in *abcam®*.
100. Bentzinger, C.F., et al., *Fibronectin regulates Wnt7a signaling and satellite cell expansion.* Cell Stem Cell, 2013. **12**(1): p. 75-87.
101. Boldrin, L. and J.E. Morgan, *Grafting of a single donor myofibre promotes hypertrophy in dystrophic mouse muscle.* PLoS One, 2013. **8**(1): p. e54599.
102. Collins, C.A., et al., *A population of myogenic stem cells that survives skeletal muscle aging.* Stem Cells, 2007. **25**(4): p. 885-94.
103. Boldrin, L. and J.E. Morgan, *Modulation of the host skeletal muscle niche for donor satellite cell grafting.* Methods Mol Biol, 2013. **1035**: p. 179-90.
104. Kirkpatrick, L.L., K.A. McIlwain, and D.L. Nelson, *Alternative splicing in the murine and human FXR1 genes.* Genomics, 1999. **59**(2): p. 193-202.
105. Wernig, G., et al., *The vast majority of bone-marrow-derived cells integrated into mdx muscle fibers are silent despite long-term engraftment.* Proc Natl Acad Sci U S A, 2005. **102**(33): p. 11852-7.
106. *What is the molecular weight of Product C9759, Cardiotoxin?*, in *Sigma-Aldrich*. 2008.
107. Rudnicki, M.A., et al., *Inactivation of MyoD in mice leads to up-regulation of the myogenic HLH gene Myf-5 and results in apparently normal muscle development.* Cell, 1992. **71**(3): p. 383-90.
108. Winokur, S.T., et al., *Expression profiling of FSHD muscle supports a defect in specific stages of myogenic differentiation.* Hum Mol Genet, 2003. **12**(22): p. 2895-907.
109. Velu, C.S. and H.L. Grimes, *Utilizing antagomiR (antisense microRNA) to knock down microRNA in murine bone marrow cells.* Methods Mol Biol, 2012. **928**: p. 185-95.
110. Cheever, A., E. Blackwell, and S. Ceman, *Fragile X protein family member FXR1P is regulated by microRNAs.* Rna, 2010. **16**(8): p. 1530-9.
111. Whitcomb, E.A., et al., *Novel control of S phase of the cell cycle by ubiquitin-conjugating enzyme H7.* Mol Biol Cell, 2009. **20**(1): p. 1-9.
112. Hall, J.K., et al., *Prevention of muscle aging by myofiber-associated satellite cell transplantation.* Sci Transl Med, 2010. **2**(57): p. 57ra83.